Phase II of the DUNE Experiment: Scientific Opportunities, Detector Concepts and Technological Challenges

The DUNE Collaboration

April 2023

Contents

1 DUNE and the Elements of DUNE Phase II

The DUNE at the Long-Baseline Neutrino Facility (LBNF) was conceived in 2015, following the recommendations of the 2013 update of the European Strategy for Particle Physics [1] and of the 2014 Report of the US Particle Physics Project Prioritization Panel (P5) [2]. The 2014 P5 Report recommended developing, in collaboration with international partners, a coherent long-baseline neutrino program hosted at Fermilab, with a mean sensitivity to CP violation of better than 3σ over more than 75% of the range of possible values of the unknown CP-violating phase δ_{CP}. Estimates at the time suggested that a 600 kt·MW·yr exposure at the Far Detector (FD) would be needed in order to reach this goal[1], together with a control of systematic uncertainties at the percent level thanks to near detector (ND) data constraints. The 2014 P5 Report also recommended a broad program of neutrino astrophysics and physics beyond the Standard Model (BSM) as part of DUNE, including demonstrated capability to search for supernova (SN) bursts and for proton decay. Likewise, the 2013 Update of the European Strategy for Particle Physics and its 2020 Update recommended the Europe and CERN (through its Neutrino Platform) should continue to collaborate towards the successful implementation of LBNF and DUNE.

Today, the vision put forward by the above strategic recommendations is still very appropriate and timely. The DUNE Collaboration and the LBNF team have made major progress toward the realization of this project, with the aim to start the scientific exploitation in 2029. Based on recent estimates, the ultimate CP violation measurement goal put forward by the

[1]The exposure is expressed here as the product of FD fiducial mass, beam power and FD exposure time.

2014 P5 Report should be reachable with an exposure of about 1000 kt·MW·yr, or about 15 years of physics data-taking. DUNE's neutrino astrophysics and BSM physics programs also require operations for at least 15 years, until the 2045 timeframe and possibly beyond.

For the successful implementation of DUNE/LBNF, the full extent of the available resources and funding profiles, a realistic estimate of the project costs, and a clear understanding of the experimental configurations and exposures that are necessary to reach various physics milestones, are all elements to be taken into consideration. As a result of this exercise, the DUNE Collaboration and the LBNF team have decided to pursue the experiment in two phases, as summarized in Table 1.

Parameter	Phase I	Phase II	Impact
FD mass	20 kt fiducial	40 kt fiducial	FD statistics
Beam power	up to 1.2 MW	2.4 MW	FD statistics
ND config	ND-LAr, TMS, SAND	ND-LAr, ND-GAr, SAND	Syst. constraints

Table 1: A high-level description of the two-phased approach to DUNE. ND-LAr, including the PRISM movement capability, and SAND are present in both phases of the ND.

The overall project design status for **Phase I** is essentially completed, and this project phase is fully funded. Excavation at the far site, as well as fabrication of various beamline and detector components for Phase I, are well underway. An important strategy for the DUNE experiment is that the LBNF facilities at both the near and far sites should fully support the full scope of the DUNE experiment from the beginning. As a consequence, during Phase I, the facilities at the near site are constructed to support a 2.4 MW primary and neutrino beamline, as well as underground near detectors for all DUNE experimental phases. Likewise, the far site will include surface and underground facilities, as well as support for four FD modules, already in Phase I. The Phase I neutrino beamline will consist of a wideband neutrino beam with up to 1.2 MW beam power, and designed to be upgradeable to 2.4 MW. The Phase I near detector will include an on-axis magnetized neutrino detector (SAND), and an off-axis LArTPC with pixel readout (ND-LAr) followed by a muon spectrometer (TMS), see [3]. Both ND-LAr and TMS are movable over a range of off-axis angles (PRISM concept), for a better characterization of the neutrino flux and neutrino-argon interactions. The Phase I far detector will include two LArTPC modules, consisting of 17 kton of liquid argon each. The FD1 module will be a horizontal drift TPC, and will be similar in concept to the ICARUS and MicroBooNE detectors, see [4]. The FD2 module will be a vertical drift TPC, and its design capitalizes on the experience with the ProtoDUNE demonstrators at the CERN Neutrino Platform. For the cryogenic infrastructure in support of the two LArTPC modules, Phase I will include two large cryostats (one per FD module), 35 kton of liquid argon, and 3 nitrogen refrigeration units.

For the **Phase II** of the experiment, several options are under consideration for the near detector, far detector and beamline designs. Nevertheless, several Phase II key elements have already been defined. The Phase II neutrino beamline will include a 2.4 MW capable target and new magnetic focusing horns, a new decay pipe window, as well as additional cooling and instrumentation. This document deals primarily with the Phase II neutrino detectors, at both the far and near sites. On the one hand, Phase II will include a more capable near detector.

The main improvement to the near detector suite for Phase II is expected to be the addition of a high-pressure argon gas TPC that is magnetized, and surrounded by an electromagnetic calorimeter and by a muon detector (ND-GAr). Upgrades to the ND-LAr and SAND systems are also possible. On the other hand, two additional FD modules will be added at the far site, for a total of four FD modules. The cryogenic infrastructure at the far site will be upgraded for Phase II with a fourth nitrogen refrigeration unit and additional 35 kton of liquid argon.

This document is organized as follows. Section 2 covers the science that will be pursued with Phase II, in the areas of long-baseline neutrino oscillation physics, neutrino astrophysics and astroparticle physics, and BSM physics. A progress report on DUNE's Phase II far and near neutrino detectors is given in Sections 3 and 4, respectively. These two sections will cover our current understanding of the detector requirements to carry out the Phase II physics goals, and a current snapshot of the main detector design options that are under consideration. These sections will also summarize the critical R&D elements that remain to be validated, and the prototyping phases to be realized, before Phase II detector construction can begin.

2 DUNE Phase II Physics

2.1 Long-baseline Neutrino Oscillation Physics

DUNE is designed to measure electron (anti)neutrino appearance and muon (anti)neutrino disappearance, as a function of (anti)neutrino energy in a wideband beam. DUNE is sensitive to all the parameters governing $\nu_1 - \nu_3$ and $\nu_2 - \nu_3$ mixing in the three-flavor model: θ_{23}, θ_{13}, Δm^2_{32} (including its sign, which is the neutrino mass ordering), and δ_{CP}.

In Phase I, DUNE can accumulate approximately 100 kt·MW·yr of data in five years. This corresponds to roughly 400 ν_e and 150 $\bar{\nu}_e$ candidates in the FD, depending on the true oscillation parameters. While DUNE will still be statistically limited, this is sufficient to conclusively determine the neutrino mass ordering at $> 5\sigma$ significance, regardless of the true parameter values. If CP violation is nearly maximal ($\delta_{CP} \sim \pm\pi/2$), DUNE can establish CP violation at 3σ in Phase I. DUNE will also make measurements of the disappearance parameters Δm^2_{32} and $\sin^2 2\theta_{23}$ that improve upon current uncertainties. However, the statistics of Phase I are too low to determine the octant of θ_{23}, or to establish CP violation except in the luckiest scenario.

The oscillation physics goals of Phase II are to make high precision measurements of all four parameters including δ_{CP}, to establish CP violation at high significance over a broad range of possible values of δ_{CP}, and to test the three-flavor paradigm as a way to search for new physics in neutrino oscillations. To do this requires $600-1000$ kt·MW·yr of data statistics depending on the measurement. This can be achieved with 6-10 additional calendar years with 2.4 MW and 40 kton fiducial mass, but would require 24-40 additional years without doubling neither the FD mass nor the beam intensity. The high precision measurements also require unprecedented systematic constraints, which may require a more capable ND. The significance for DUNE to establish CP violation is shown as a function of time in Figure 1.

With Phase II, DUNE can establish CP violation at $> 3\sigma$ over 75% of possible δ_{CP} values, and measure the δ_{CP} phase at a precision of $6 - 16^\circ$ depending on the true value. DUNE can also measure θ_{23} with world-leading precision and determine the octant if it is sufficiently

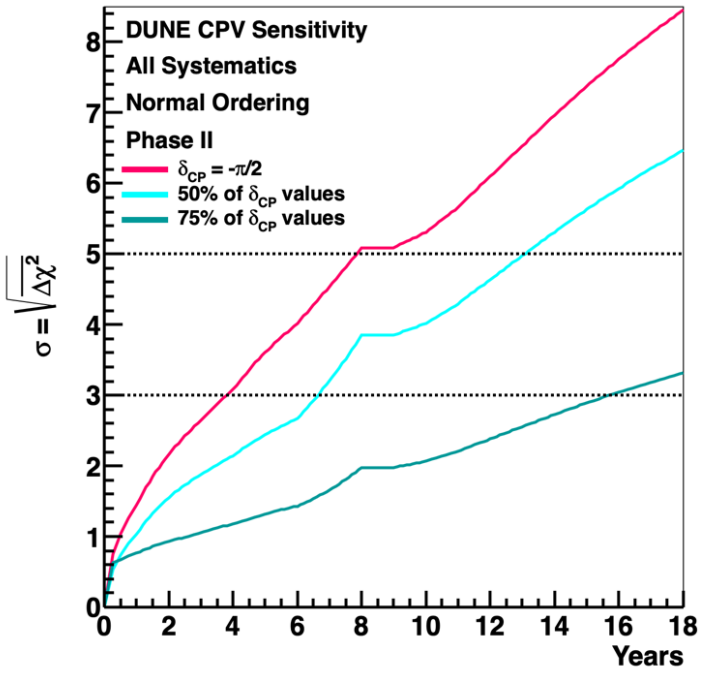

Figure 1: The significance for DUNE to establish CP violation as a function of time. Here, the initial ramp up exceeds 1.2 MW due to Fermilab's Accelerator Complex Evolution (ACE) upgrades to the Main Injector [5]. The Phase II ND is assumed to be complete by year 6, and year 8 is a shutdown to replace the Booster, after which the ultimate 2.4 MW beam power is reached. The third and fourth FD modules are assumed to turn on after years 3 and 5, respectively.

non-maximal. The measurements of θ_{13} and Δm^2_{32} will approach the precision of the current measurement from Daya Bay and the planned measurement from JUNO, respectively, but are made with a different neutrino flavor and helicity, over a different baseline, and at a different energy, such that comparisons between experiments test the three-flavor model. DUNE is also sensitive to physics beyond the Standard Model that impacts neutrino oscillations, including non-unitary mixing, non-standard interactions, CPT violation, and additional neutrino species (see Sec. 2.3.

The increased statistics in the FD are achieved with two additional modules, FD-3 and FD-4. It is crucial that the data from these modules be combined with data from FD-1 and FD-2, and that the ND constraints apply to all FD modules. For this reason, the most straightforward approach is for FD-3 and FD-4 to be LArTPCs, which would immediately benefit from the ν-Ar measurement program of the ND. Depending on the ultimate performance of the Phase I ND, an upgrade may be required to achieve the required level of systematics for Phase II, so that the analysis is not systematically limited. This is the role of the more capable Near Detector (see Sec. 4.1), which would replace the muon spectrometer with a detector that adds to the

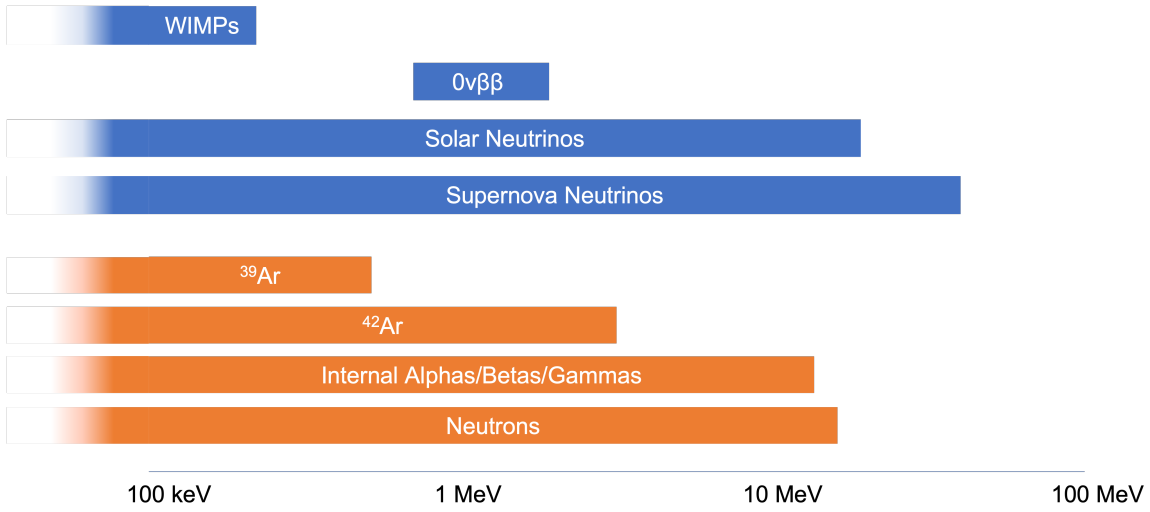

Figure 2: Visible energy ranges in DUNE for potential <100 MeV signatures of astrophysical or other beam-unrelated origin (blue), together with relevant backgrounds (orange). From [7].

measurement program and constrains additional uncertainties, while also measuring muons from ND-LAr.

2.2 Neutrino Astrophysics and Astroparticle Physics

DUNE is designed to conduct a broad physics program, including also the detection of neutrinos from astrophysical sources in the MeV energy range [6]. DUNE's expected energy threshold is a few MeV of deposited energy, and the expected energy resolution is around 10-20% for energies in the few tens of MeV range. For a summary of neutrino astrophysics and astroparticle physics opportunities with DUNE Phase II, together with relevant backgrounds, see Fig. 2

DUNE will be part of a growing network of experiments for **multi-messenger astronomy**. Neutrinos from a **core collapse supernova** contain a wealth of information about astrophysical processes as well as particle physics. DUNE is uniquely sensitive to electron neutrinos from a galactic supernova burst with energies larger than 5 MeV [8]. Already in Phase I, DUNE will be able to detect neutrinos from a core-collapse supernova. Phase II is a fundamental step, since the precise measurement of the supernova spectral parameters and the burst trigger efficiency are dominated by the number of neutrino interactions in the detectors. While the expected event rate varies significantly among models of supernova explosions, the 40-kt (fiducial) DUNE detector would be expected to observe approximately 3000 neutrinos from a supernova burst at 10 kpc. DUNE will have sensitivity to several supernova observables (information about the progenitor, the collapse, the explosion, and the remnant), as well as information about neutrino properties by detecting the flavor content and spectra of neutrinos throughout the supernova evolution phases. The neutrino mass ordering has a strong impact on the expected signal at early times (neutronization burst) when the neutrino flux is dominated by electron neutrinos. Neutrino flavor transformation probabilities can be affected by neutrino-neutrino scattering and

collective modes of oscillation. These effects will leave imprints on the neutrino signal and can be used to study these phenomena experimentally. DUNE is also able to provide competitive constraints on the absolute neutrino mass via time of flight measurements [9].

Neutrinos and antineutrinos from other astrophysical sources, such as **solar neutrinos** [10] and the **diffuse supernova neutrino background** are potentially detectable although challenging, particularly because of the presence of radioactive backgrounds in the detector. Initial studies suggest potential for DUNE to select a sample of solar neutrinos that would allow a significant improvement in the measurement of Δm^2_{21} as well as a first observation at $>5\sigma$ of the hep solar neutrino flux (that is, neutrinos produced via the ^{3}He + p $\rightarrow$ ^{4}He + e$^+$ + ν_e nuclear fusion reaction in the Sun's interior). More capable detectors in Phase II with improved reconstruction, energy resolution, calibration, timing, and most importantly lower background levels would enhance the DUNE low-energy physics reach.

Even lower neutrino detection thresholds and background rates would expand DUNE's physics reach further, including the possibility to search for WIMP dark matter, neutrinoless double beta decay or CEνNS interactions at the FD. This would imply additional capabilities and important innovations for the current far detector technologies, see Sec. 3. Table 2 lists some of the physics topics that could be accessible in an expanded DUNE Phase II program, along with the detector performance requirements.

Table 2: Physics topics accessible in DUNE Phase II, with requirements for performance beyond the reference LAr-TPC design.

Physics Topic	**Physics Goal**	**Requirements**
Long-baseline oscillations	CPV	Achieved in reference design
Supernova burst	ν detection	Reference design
	$\bar{\nu}$ detection	IBD sensitivity
	pointing accuracy	ES sensitivity
Diffuse Supernova Neutrino Background		Neutron shielding
Solar neutrinos	CNO neutrino flux	Radio purity, neutron shielding, low threshold
	MSW transition	Radio purity, neutron shielding, low threshold
Reactor neutrinos	Standoff demonstration	Radio purity, neutron shielding, low threshold
Geo neutrinos	Flux, U/Th ratio	Radio purity, neutron shielding, low threshold
NLDBD	Majorana ν	Excellent MeV-scale energy resolution
		Radio purity, neutron shielding, low threshold
Nucleon decay	Invisible modes	Radio purity, neutron shielding, low threshold

2.3 Beyond the Standard Model Physics

DUNE's sensitivity to Physics Beyond the Standard Model (BSM) offers the ability to significantly constrain models and the potential for paradigm-changing discoveries that are complementary to those at collider experiments and other precision experiments. DUNE can probe

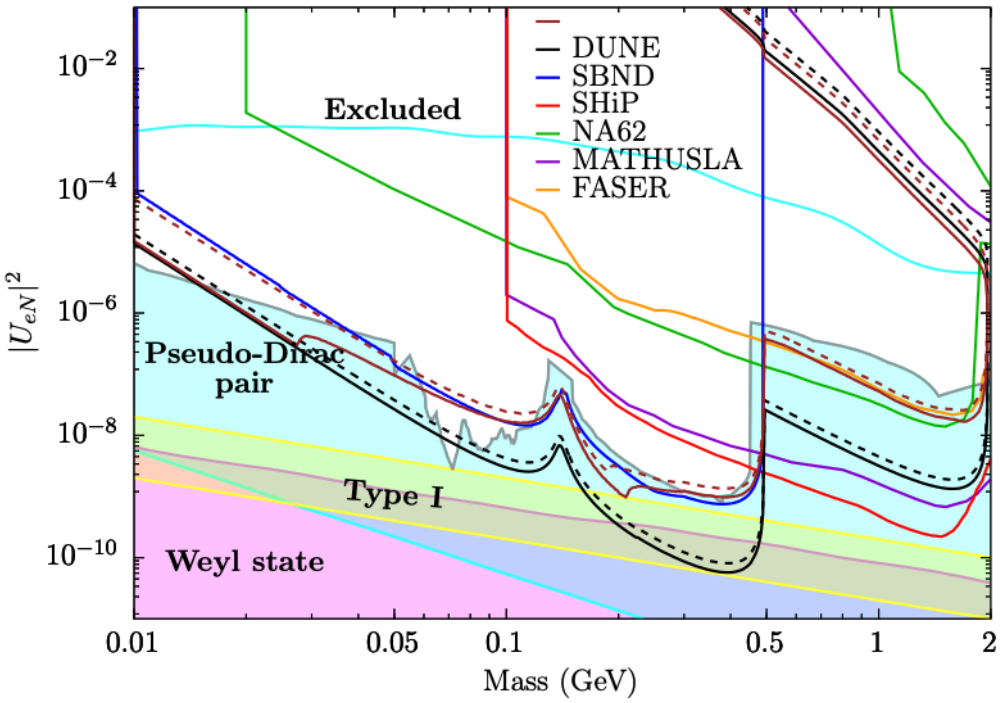

Figure 3: Heavy neutral lepton 90% C.L. sensitivity regions for $|U_{eN}|^2$ dominant mixing. The study is performed for Majorana neutrinos (solid) and Dirac neutrinos (dashed), in the case of no background (black) and after a basic background analysis (brown). The DUNE analysis (black) is compared to no background sensitivities from other future experiments, shown in the other colored lines. The yellow band represents the phase space predicted by Type I seesaw models [12].

a diverse range of BSM phenomenology, including searches for dark matter, sterile neutrino mixing, non-standard neutrino interactions, CPT violation, new physics enhancing neutrino trident production, baryon number violating processes, and neutrino oscillation physics beyond the three neutrino paradigm [11].

Beyond the Standard Model physics accessible at DUNE may be divided into three major areas of research: rare event BSM particle searches at the ND, rare event BSM particle searches at the FD, and non-standard neutrino oscillation phenomena. In the following, we give examples where DUNE Phase II will bring additional unique sensitivity with respect to Phase I and to the current state of the art.

The high intensity of the LBNF neutrino beam and the production of charm mesons in the beam enables DUNE to search for a wide variety of long-lived, exotic, particles with the ND. In Phase II, the low-density ND-GAr adds additional unique sensitivity to any BSM search involving neutral particles produced in the beam and decaying in the ND. For decay signatures, the BSM signals are proportional to the detector active volume, while backgrounds from neutrino interactions are proportional to detector mass, hence low-density detectors such as ND-GAr provide a favorable signal-to-background ratio. Searches for heavy (up to $\approx$0.5 GeV)

neutral leptons (HNLs) and heavy axions are thus particularly well motivated during DUNE Phase II. For HNLs, the decay rates are proportional to $|U_{\alpha N}|^2$ in the case of single dominant mixing, where $\alpha = e, \mu, \tau$. Figure 3 shows the combined sensitivity for HNL decay channels sensitive to $|U_{eN}|^2$ only, as a function of HNL mass [12]. As can be seen from the figure, DUNE is world-leading at masses below ≈0.5 GeV, complementary to the LHC heavier mass searches. In addition, DUNE may have the potential to explore some phase space predicted by Type I seesaw models. Other phenomenological studies [13, 14] confirm the potential of the DUNE Phase II ND for HNL searches. Similarly to the HNL case, the DUNE Phase II ND is also uniquely sensitive to axions with masses between 20 MeV and 2 GeV, see [15, 16].

Another rare event search at the ND is neutrino trident production. Neutrino trident production, that is, the production of a pair of oppositely-charged leptons through the scattering of a neutrino on a heavy nucleus, is a powerful probe of BSM physics in the leptonic sector [17, 18]. The Standard Model expectation is that the ND will collect around a dozen of these rare events per ton of argon per year, enough to measure with precision the cross-sections of such processes [19, 20]. To date, only the dimuon final-state has been observed, although with considerable uncertainties. The main challenge in obtaining a precise measurement of the dimuon trident cross-sections ($\nu_\mu \to \nu_\mu \mu^+ \mu^-$ and $\bar{\nu}_\mu \to \bar{\nu}_\mu \mu^+ \mu^-$) at DUNE will be the copious backgrounds, mainly consisting of charged-current single-pion production events ($\nu_\mu N \to \mu \pi N'$), as muon and pion tracks can be easily confused. ND-GAr will tackle this search by improving muon-pion separation through dE/dx measurements in the high-pressure gas TPC and the calorimeter system, and ND-GAr's magnetic field will significantly improve signal-background separation by tagging the opposite charges of the two muons in the final state. While the TMS muon spectrometer system in Phase I will have some muon momentum and charge sign measurement capabilities, the Phase II ND will greatly extend those, particularly in the $E_\mu \gtrsim 6$ GeV muon phase space region, which is relevant for this search.

Regarding rare event, beam-unrelated, BSM particle searches at the FD, the Phase II will be particularly beneficial for searches that are expected to be virtually background-free at the scale of the experiment's full exposure. In such ideal cases, the decay or scattering rate sensitivity will be inversely proportional to the FD exposure (in kt·yr), and Phase II exposure will make a crucial difference. Background-free (or quasi-background.-free) searches at the FD may include baryon number violating processes. For example, current estimates [11] for the $p \to K^+ \bar{\nu}$ search yield a mean background rate expectation of 0.4 events for a 400 kt·yr exposure at the FD. Searches for baryon number violating processes with different final states may also be background-free in DUNE, and will be explored during Phase II.

Possible non-standard neutrino oscillations at both FD and ND will be probed during Phase II. The access to non-standard oscillation phenomena would be boosted by adding tau neutrino appearance channels to DUNE's standard electron neutrino appearance and muon neutrino disappearance channels. At the FD, the observation of anomalous ν_τ appearance may point to mixing with heavy neutral leptons or to non-standard neutrino interactions [21, 22]. At the ND, the observation of any ν_τ appearance may point to short-baseline $\nu_\mu \to \nu_\tau$ oscillations and to light sterile neutrino mixing. DUNE's Phase II beam and detectors may offer unique opportunities for tau neutrino appearance searches. First, DUNE will have the capability to run during Phase II with a higher energy beam tune optimized for ν_τ detection above the τ

production threshold ($E_\nu \gtrsim 3.4$ GeV). Studies indicate that the ν_τ charged-current interaction rate may almost double at the FD in this case, compared to the standard LBNF/DUNE beam optimized for CP violation, see [23]. Also, ν_τ charged-current interaction topologies will be challenging to reconstruct and select in DUNE's Phase I detectors. Several τ decay modes exist, in many cases with complicated hadronic final states that need to be fully reconstructed and separated from the remaining neutrino interaction hadronic products. DUNE FD modules with improved tracking capabilities, for example via a pixelated readout, may provide significantly better efficiencies and purities for the study of tau neutrino appearance. At the ND, ND-GAr will provide improved acceptance for tau decay muons, particularly for the high-energy ($E_\mu \gtrsim 6$ GeV) ones, largely improving DUNE's Phase I reach for light sterile neutrinos that mix with the tau sector.

3 The DUNE Phase II Far Detector

The primary objective of the DUNE Phase II Far Detector is to increase the fiducial mass of DUNE to at least the originally planned 40 kton. For long-baseline neutrino oscillations, it is critical that all four FD modules are compatible with the systematic constraints of the Near Detector. Non-LAr options for the Phase II FD would require corresponding additions or changes to the ND complex in order to achieve a comparable level of systematic uncertainty.

For MeV-scale physics, the additional mass would double the statistics of a supernova burst and extend the reach beyond the Milky Way. An exposure of hundreds of kton-yrs is required to improve upon oscillation parameter measurements with solar neutrinos. Most BSM searches also require very long exposures to be competitive.

Enhancements to the detector design have the potential to improve the DUNE program, including by lowering the threshold for MeV-scale neutrinos. Phase II also presents opportunities to expand the DUNE science program to new areas while preserving the essential core measurement capabilities.

3.1 The first DUNE Vertical Drift Far Detector

The vertical drift detector as implemented in ProtoDUNE-VD and planned for FD2 (Figures 4 and 5) draws from the strengths of DUNE ProtoDUNE-DP and ProtoDUNE-SP as well previous horizontal drift detectors: ICARUS and MicroBooNE. The vertical drift design simplifies detector construction and installation, reducing overall detector costs relative to the well-established single-phase (SP) horizontal drift design based on large wire plane assemblies. The vertical drift detector uses most of the same structural elements as DP (e.g., the top charge-readout planes (CRPs) that form the upper anode plane and the field cage that hangs from the cryostat roof) and is constructed of modular elements that are easy to produce, transport and install.

The cathode at the vertical mid-plane of the detector is suspended from the top CRP support structure and subdivides the detector into two vertically stacked drift volumes of 6.5 m height each, with CRP readout for both the top and bottom drift volumes. The top CRPs are suspended from ports on the cryostat roof and are readout via the top drift electronics (TDE)

Figure 4: Schematic of vertical drift concept with PCB-based charge readout. Corrugations on cryostat wall shown in yellow; PCB-based CRPs (brown, at top and bottom with superstructure in gray for top CRPs); cathode (violet, at mid-height with openings for photon detectors); field cage modules (white) hung vertically around perimeter (70% transparent portion in regions near anode planes); photon detectors, placed in the openings on the cathode and on the cryostat walls, around the perimeter in the vertical regions near the anode planes.

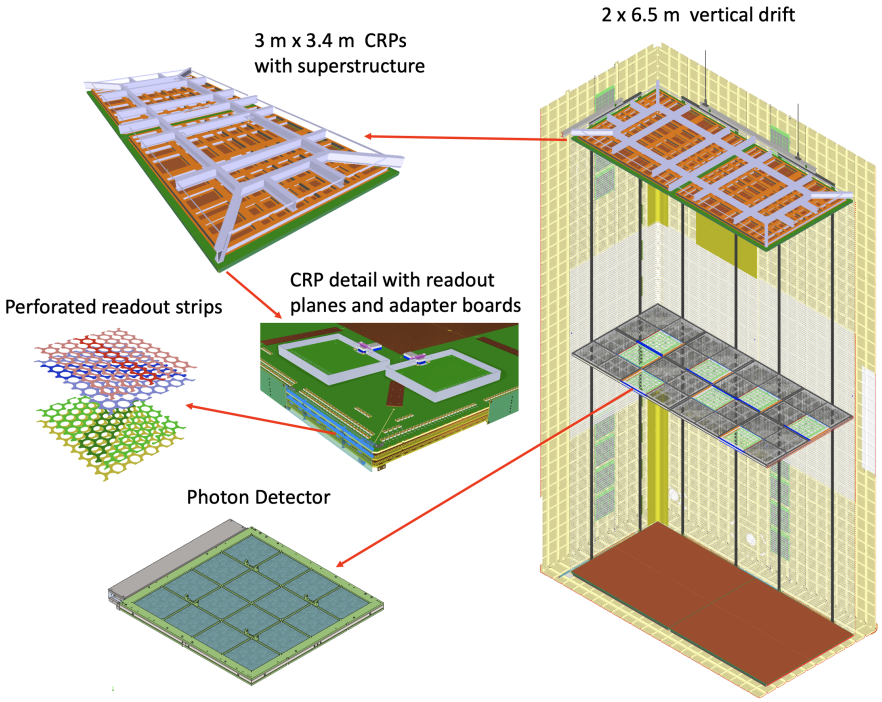

via signal feedthrough chimneys (SFT chimneys) on the roof and are fully accessible for repair or upgrade as in ProtoDUNE-DP. The bottom CRPs are supported by feet on the cryostat floor and are readout via the bottom drift electronics (BDE) (using the same cold electronics (CE) as in ProtoDUNE-SP).

The important features of the vertical drift design are listed here:

- maximize the active volume;
- high modularity of detector components;
- simplified anode structure based on standard industrial techniques;
- simplified cold testing of instrumented anode modules in modest size cryogenic vessels;
- field cage structure independent of the other detector components;
- extended drift distance;
- reduction of dead material in the active volume;

Figure 5: Perspective view of the vertical drift detector module (FD2-VD) detector.

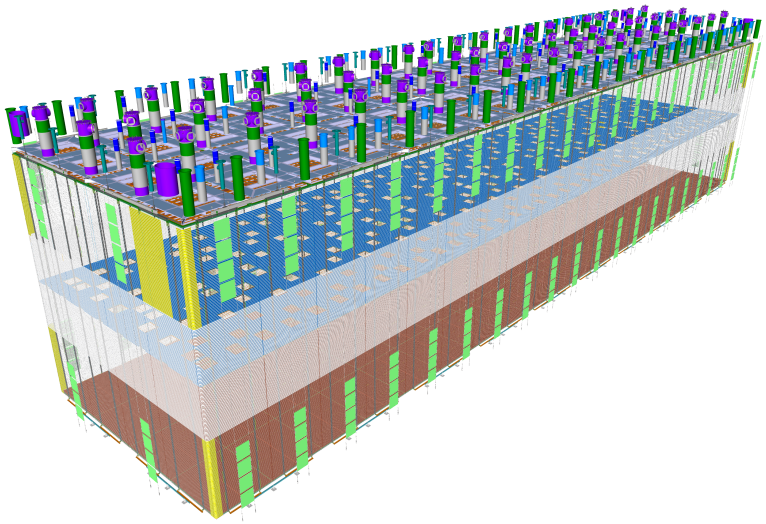

- design allowing for improved light detection coverage;
- simplified and faster installation and quality assurance (QA)/quality control (QC) procedures; and
- cost-effectiveness.

3.1.1 Charge Readout Planes (Anodes)

The baseline design FD2-VD anodes, illustrated in Figure 6, are fabricated from two double-sided perforated PCBs, 3.2 mm thick, that are connected mechanically, with their perforations aligned, to form charge-readout units (CRUs). A pair of CRUs is attached to a composite frame to form a CRP; the frame provides mechanical support and planarity. The holes allow the electrons to pass through to reach the collection strips. Each anode plane consists of 80 CRPs in the same layout. The CRPs in the top drift volume, operating completely immersed in the LAr, are suspended from the cryostat roof using a set of superstructures, and the bottom CRPs are supported by posts positioned on the cryostat floor. The superstructures hold either two or six CRPs, and allow adjustment, via an externally accessible suspension system, to compensate for possible deformations in the cryostat roof geometry.

The FD2-VD top and bottom drift volumes implement different charge readout (CRO) electronics, top drift electronics (TDE) and bottom drift electronics (BDE), in order to take maximal advantage of placement of the top anode near the cryostat roof and to leverage the local amplification an digitization of the signal on the bottom anode to maximize the signal to noise. The TDE, based on the design used in ProtoDUNE-DP, has both cold and warm

Figure 6: A top superstructure (green structure on top) that holds a set of six CRPs, and below it an exploded view of a CRP showing its components: the PCBs (brown), adapter boards (green) and edge connectors that together form a CRU, and composite frame (black and orange).

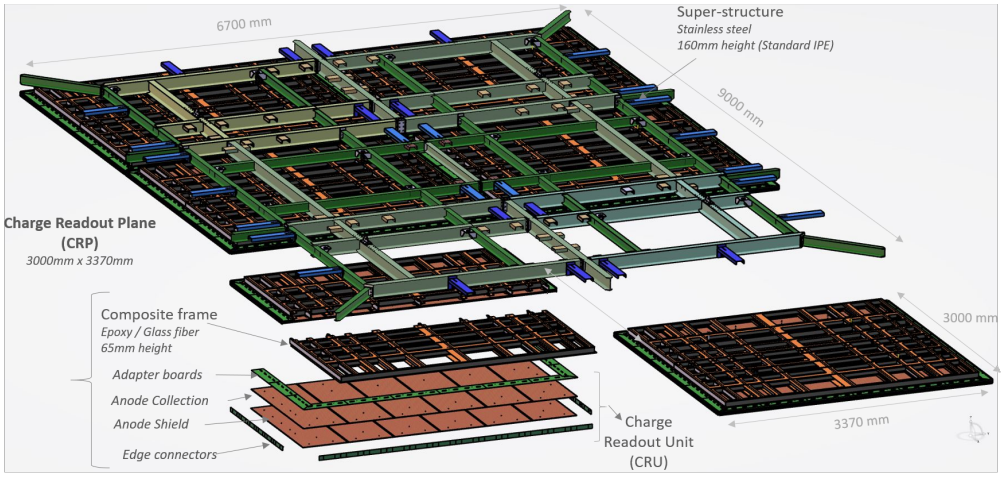

components. The BDE optimizes signal to noise with the same CE used in the FD1-HD with signal processing and digitization on the CRP in the LAr.

3.1.2 High Voltage System

The DUNE FD2-VD detector module design, which includes two drift volumes of equal drift distance 6.5 m and a nominal uniform E field of 450 V/cm, has a horizontal cathode plane placed at detector mid-height held at a negative voltage and horizontal anode planes (biased at near-ground potentials) at the top and bottom of the detector. The main high voltage system (HVS) components are illustrated in Figure 7.

The HVS is divided into two systems: (1) supply and delivery, and (2) distribution. The supply and delivery system consists of a negative high voltage power supply (HVPS), HV cables with integrated resistors to form a low-pass filter network, a HV feedthrough (HVFT), and a 6 m long extender inside the cryostat to deliver −294 kV to the cathode. The distribution system consists of the cathode plane, the field cage, and the field cage termination supplies. The cathode plane is an array of 80 cathode modules, with the same footprint as the CRPs, formed by highly resistive top and bottom panels mounted on fiber-reinforced plastic (FRP) frames. The modular field cage consists of horizontal extruded aluminum electrode profiles stacked vertically at a 6 cm pitch. A resistive chain for voltage division between the profiles provides the voltage gradient between the cathode and the top-most and bottom-most field-shaping rings.

In addition to the primary function of providing uniform E fields in the two drift volumes, both the cathode and the field cage designs are tailored to accommodate photon detection system (PDS) modules (Section 3.1.3) since it is not possible to place them behind the anode plane, as in the FD1-HD design. Each cathode module is designed to hold four double-sided

Figure 7: A birds-eye view of the field cage, with one full-height field cage column (highlighted in cyan) that extends the entire height, the HV feedthrough and extender (in the foreground), and the cathode (with one cathode module highlighted in cyan and X-ARAPUCA modules installed on cathode).

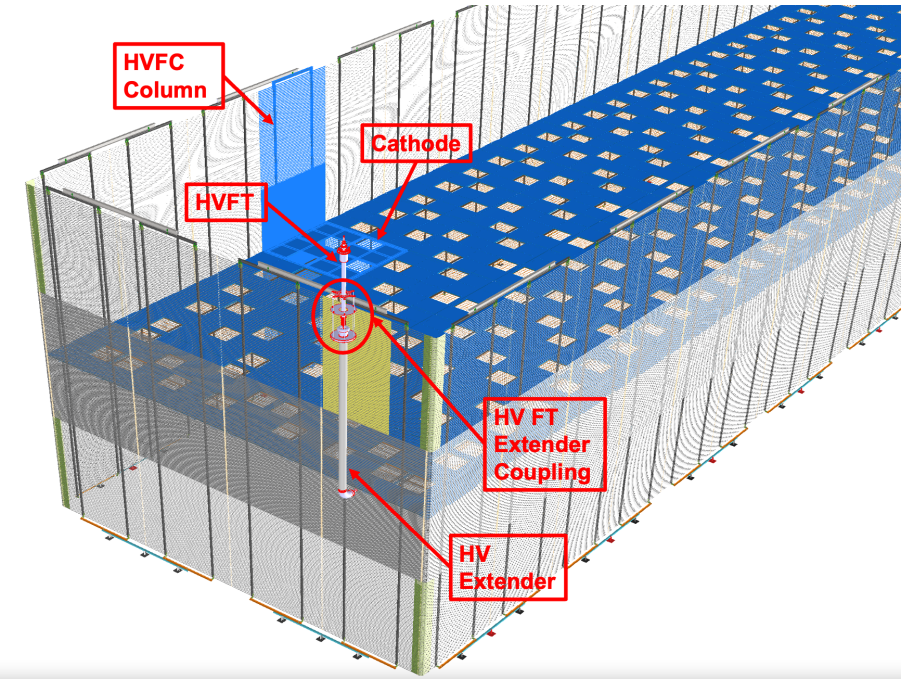

X-ARAPUCA PDS modules that are exposed to the top and bottom drift volumes through highly transparent wire mesh windows. Along the walls, the field cage is designed with narrower profiles in the region within 4 m of the anode plane to provide 70% optical transparency to single-sided PDS mounted on the cryostat membrane walls behind them, and conventional-width profiles within 2 m of the cathode plane.

3.1.3 Photon Detection System

The FD2-VD will implement X-ARAPUCA [**?**, **?**] PDS. Functionally, an X-ARAPUCA module is a light trap that captures wavelength-shifted photons inside boxes with highly reflective internal surfaces until they are eventually detected by silicon photomultipliers (SiPMs). An X-ARAPUCA module has a light collecting area of approximately $600 \times 600\,\mathrm{mm}^2$ and a light collection window on either one face (for wall-mount modules) or on two faces (for cathode-mount modules). The wavelength-shifted photons are converted to electrical signals by 160 SiPMs distributed evenly around the perimeter of the photon detector (PD) module. Groups of SiPMs are electrically connected to form just two output signals, each corresponding to the sum of the response of 80 SiPMs.

Since their primary components are almost identical to those of FD1-HD, only modest R&D was required for the FD2-VD PDS m]odules. The primary differences were to optimize the module geometry and the proximity of the SiPMs to the wavelength-shifting (WLS) plates. Both of these are more favorable in FD2-VD, leading to more efficient light collection onto the SiPMs. As discussed in Section 3.1.2, the design has the PDs mounted on the four cryostat membrane walls and on the cathode structure, facing both top and bottom drift volumes. This configuration produces approximately uniform light measurement across the entire TPC active volume.

Cathode-mount PDs are electrically referenced to the cathode voltage, avoiding any direct path to ground. While membrane-mount PDs adopt the same copper-based sensor biasing and readout techniques as in FD1-HD, cathode-mount PDS required new solutions to meet the challenging constraint imposed by HVS operation. The cathode-mount PDS are powered using non-conductive power-over-fiber (PoF) technology [**?**], and the output signals are transmitted through non-conductive optical fibers (signal-over-fiber (SoF)), thus providing voltage isolation in both signal reception and transmission.

3.1.4 Upgrade path from FD2 to Phase II Vertical Drift

Several variations on the vertical drift design are under consideration to improve performance or reduce cost. These improvements are broadly grouped into two classes: optimization of the charge readout and optimization of the photon readout system.

Optimizations of the charge readout system include options to improve the production processes and reduce the cost of the CRPs, possible optimizations of strip pitch and length and channel count. Other options are to replace the strip based CRP with a pixel based CRP or with an optical readout based on electroluminescence.

Optimizations of the photon readout include two broad classes. One of the most attractive options is the proposed Aluminum Profiles with Embedded X-arapuca (APEX) concept in

Section 3.2.1 where photon detectors are integrated into the field cage. The developed PoF and SoF technologies in FD2 open up the opportunity to extend toward a 4π optical coverage in the FD module. The other class of optimization is the addition of photon detection to a pixel-based CRP.

3.2 Optimized Vertical Drift Far Detector Module for DUNE Phase-2

An optimized version of the vertical drift LArTPC design, developed for Phase-1 FD2, is proposed here for DUNE Phase-2 FD Module(s), with some options for the charge and the light readout solutions.

3.2.1 Field Cage Integrated Large Area Photon Detection System (APEX)

The leading criteria for optimization of the light readout system proposed here for Phase II FD modules are performance enhancement at low incremental costs, leveraging on minimum risk development of solutions already demonstrated and adopted for Phase I. This is achieved by increasing toward 4π the active optical coverage of the LAr target volume with a simplified lightweight low(er)-cost photo-detector solution derived from the well-established XARAPUCA technology with SiPM photosensors developed for VD FD2. Improving light collection capability (i.e. better time resolution, higher and more uniform light yield across the LAr volume) provides a lower energy threshold, relevant for low energy physics reconstruction, and enhances energy resolution from scintillation light measurement for MeV to GeV neutrino physics analyses.

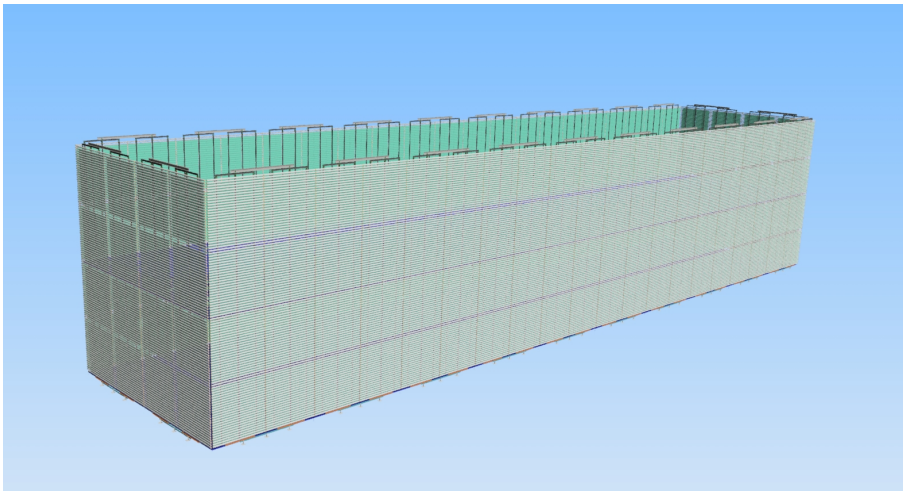

Figure 8: A bird's-eye view of the field cage with integrated large area photon detection system (APEX) for DUNE Phase II FD module(s). The FC structure is modular and made of panels vertically stacked in groups of 4 hanging from the top and all around the LAr drift volume.

The field cage, an element of the HV system, delimits the four sides of the VD LArTPC volume between the cathode and anode (top and bottom planes) and thus offers the largest available surface for extended optical coverage. Up to ∼ 60% optical coverage of the LArTPC volume can be realized in case the FC walls are fully instrumented with photodetectors integrated with the FC aluminum profile electrodes. The PD readout electronics in this case should necessarily be referenced to the (high) voltage level of the electrode profile bearing the PD module, and therefore it needs to be electrically isolated. Power and signal transmission can be established via non-conductive optical fibers, as for the photon detector of FD2 integrated on the cathode plane at very high voltage. The solution is offered by the PoF and SoF technologies developed for the DUNE vertical drift module as described in Section 3.1.3. These have been demonstrated to work reliably for electrical isolation with noise immunity and long-term stability in cold.

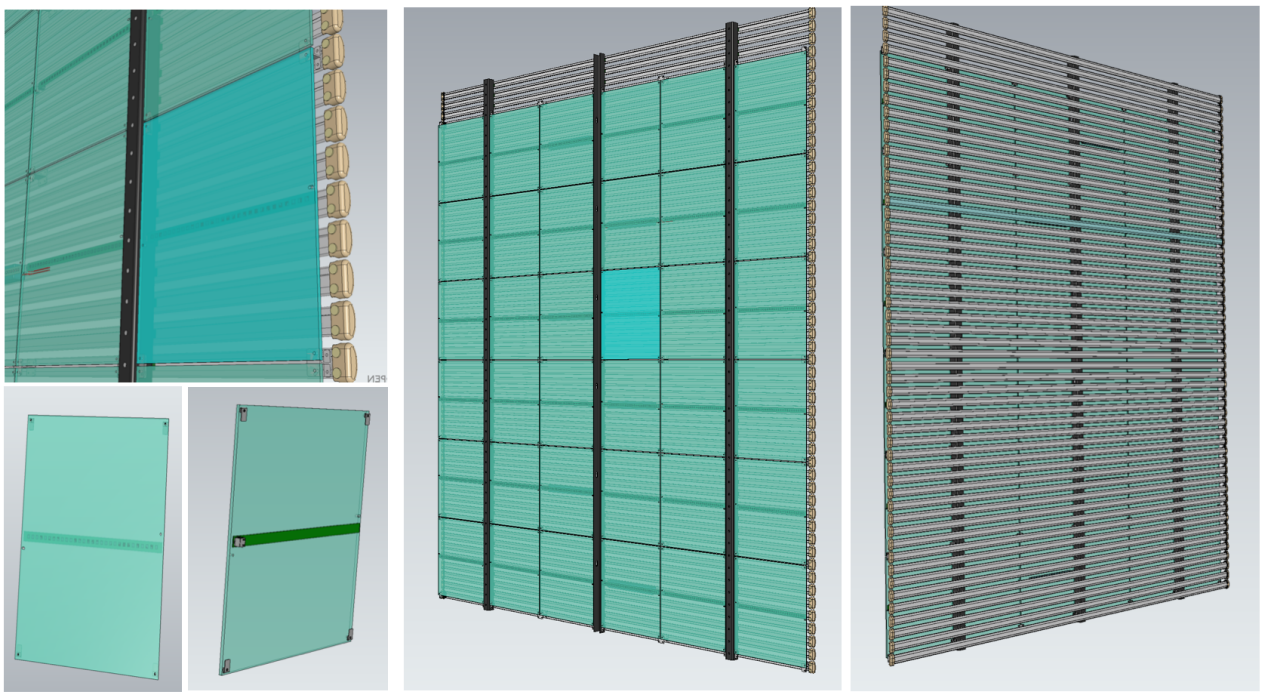

Figure 9: The APEX modular panel: details of the PD module equipped with a SiPM board at the center, a front view showing the array of PD modules, and a back view showing the FC aluminum profiles structure.

The field cage integrated large area photon detection system (hereafter dubbed APEX) for DUNE Phase II FD module(s), shown in Fig. 8 and described here below, assumes to keep the same FC structure as designed for the FD2 VD Module (see Section 3.1.3 Figure 7). This is a modular structure made of FC panels, $3.0 \times 3.2\,\mathrm{m}^2$ assemblies consisting of horizontal extruded aluminum electrode profiles (C-shaped, 3 m long and 6 cm wide) stacked vertically at a 6 cm pitch mounted on vertical FR4 I-beams. The profiles are connected by a resistive voltage divider chain setting the profile's HV level, degrading from cathode at max HV to ∼ ground at

the top-most and bottom-most field-shaping electrodes.

The modular APEX panel for Phase II FD module(s) is a standard VD FC panel equipped with a (6×6) array of thin, large area ($\sim 50 \times 50\,\mathrm{cm}^2$) ARAPUCA-type PD modules framed onto the FC structure and fully covering it, as shown in Fig. 9. The PD modules of each row of the array are mechanically fastened and electrically referenced to the horizontal aluminum profile at the mid-height of the row. The cavity of the C-shaped profile offers housing and Faraday shielding for the cold electronics readout boards of the PD modules of the row. Several PoF units and an SoF unit at the center of the 3 m long profile receive power and transmit signal for the modules of the row via optical fibers, routed in/out from the penetration at the top of the FD cryostat using the central vertical I-beam of the FC structure as fiber cable conduit, see details in Fig. 9. Each row of 6 PD modules in an APEX panel thus forms an electrically isolated system as shown in Fig. 10.

There are 192 APEX panels, stacked vertically in groups of 4 and all around the drift volume, forming the VD field cage structure for Phase II FD module(s) as shown in Fig. 8, split in 1152 PD row isolated systems, with 6 PD modules each. The number of fibers for power distribution and signal transmission depends on the electrical/electronic architecture adopted and hardware components. With the basic option of signal conditioning and digitization in cold, followed by optical conversion and SoF transmission by laser diode, as developed in the course of the R&D phase for FD2 PDS, a max number of 8 fibers per row in the APEX panel is envisaged (1 SoF + 1 PoF HV + 6 PoF LV fibers bundled in a protective tube and terminated with standard fiber-optic connector). Fiber tubes of different lengths run vertically from the feed-through flange on the top, down along the I-beam conduit to intercept and connect to the PoF/SoF units at the center of the corresponding row of PD modules in the APEX panel (9216 fibers in total).

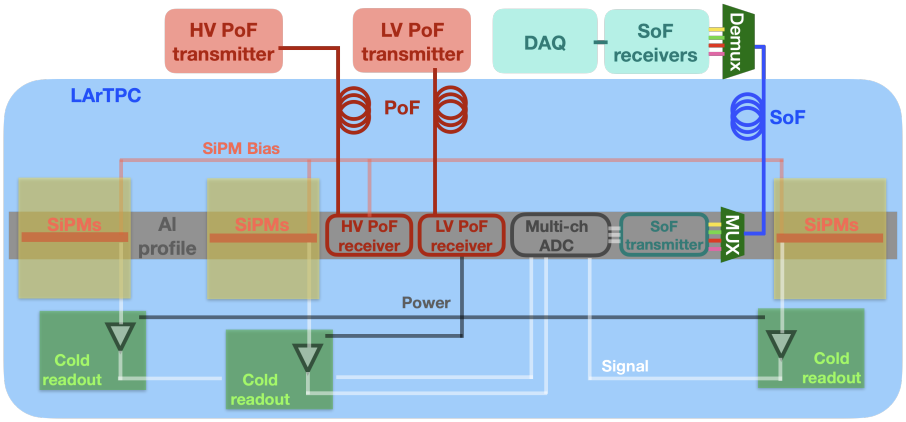

Figure 10: APEX cold readout concept: a row of 6 PD modules (only 3 are displayed) in an APEX panel forming an electrically isolated single readout system.

The PD module, elemental unit of the APEX array, is a maximally simplified application of

the light trap ARAPUCA concept, at the basis of DUNE FD1 and FD2 PDS. Two wavelength-shifting stages (WLS#1 and WLS#2), with a dichroic filter (DF) in between convert, transmit, and trap incident LAr scintillation light under the dichroic filter layer. All this is realized in a single slab, a 6 mm thick, $\sim 50 \times 50\,\mathrm{cm}^2$ flat piece of a solid PMMA (transparent acrylic), shown in Fig. 8. DF layer is directly deposited on the front plane of the acrylic substrate and the WLS #1 coating on top. Chromophore molecules embedded in the substrate PMMA (WLS#2) matrix shift transmitted light to wavelength above the DF cutoff. Light trapping is optimized by ultra-high reflectivity non-metallic thin film lamination (e.g. Vikuiti ESR) of the acrylic slab edges and backplane area. An array of SiPMs mounted on a flex PCB are optically bonded to the acrylic surface, e.g. as shown in Fig. 8. Photons trapped by reflection in the slab are eventually absorbed by the photosensors producing electronic signals digitized and transmitted out via fiber-optic. A number of 80 SiPMs per module (large area, high PDE), ganged together into one readout channel, should be sufficient to result in an overall (goal) detector efficiency of $\epsilon_D \simeq 2\%$. The PD unit is thus a lightweight ($\sim$1.8 kg), compact object conceived for fast mass production through a series of industrial fabrication processes.

Six PD modules in an APEX row input a single low-power multi-channel ADC for cold digital readout and multiplexing over a single optical fiber via SoF transmitter (driver and laser diode), as schematically represented in the block diagram of Fig. 10.

Assembly of APEX panels is expected to be uncomplicated and carried at medium/large scale university/lab experimental facilities, where FC aluminum profiles are first assembled forming the FC panel, then electronics boards positioned into the selected profiles, PD modules connected to the boards and at last fastened to the profiles, completing the APEX panel assembly, ready for transportation to the far site underground.

Bulk items of APEX assembly (aluminum profiles and acrylic plates) are intrinsic low-radioactive content materials, favoring lower background levels and thus enhancing the DUNE Phase II low energy physics reach. The general concepts of a radiopure VD-like DUNE module are detailed in section 3.3 and apply to APEX, specifically by ensuring reduced gammas and alpha-gammas internal background from the ^{232}Th and ^{238}U concentrations in the acrylic and aluminum selected materials.

A G4 simulation has been performed of a Phase II FD module with APEX optical coverage (55%) of the LAr volume. The light yield $LY(x, y, z)$ of the system was evaluated, i.e. the number of photoelectrons collected per unit of deposited energy anywhere in the LAr volume, assuming 2% detection efficiency of the ARAPUCA module and standard LAr scintillation light emission and propagation parameters. An average value $\langle LY \rangle = 181 \frac{PE}{MeV}$ across the detector volume, with a minimum of $LY_{min} = 128 \frac{PE}{MeV}$ near the anode planes are found from the simulation, as expected due to the extended optical coverage of the APEX system. In Fig.11 the LY map is in the transverse plane at the center of the FD module long axis.

A series of prototypes, from table-top size to larger sizes, cubic meters of LAr up to O(1 kTon) protoDUNE sized prototypes, are planned to fully develop and engineer the APEX concept.

A first round of prototyping aiming to study the impact on the drift field uniformity after introducing insulating material between FC electrodes has been already carried out at CERN, using a modified version of the 50lt TPC at the CERN Neutrino Platform. The expected, though

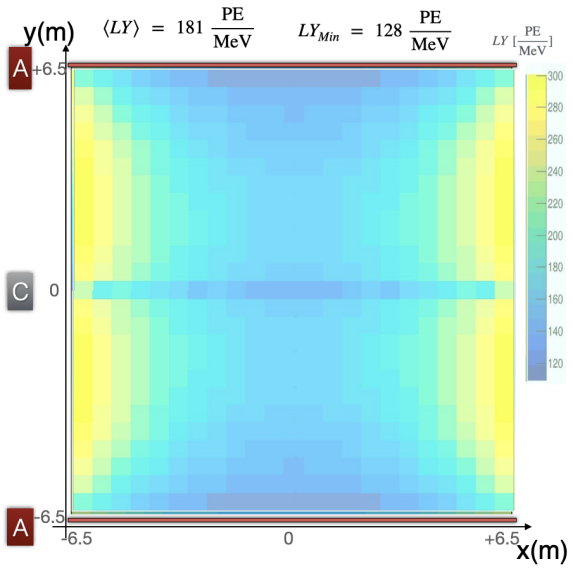

Figure 11: Map of the light yield (LY) in the central (x, y) transverse plane at $z = 0$ (G4 simulation) relative to the FC-extended coverage APEX photon detection system. Dimmer regions are near the anode planes (PD non-instrumented) at the top and bottom, and at mid-height due to the non-fully-transparent, non-instrumented cathode plane.

rather slow, buildup of static charge on the surface of insulating material has been observed. This effect can contribute to the uniformity of the electric field near the FC electrodes. This may allow - if desirable in the APEX panel design - to reduce the number of FC electrodes, with a larger pitch in between.

The 2024 calendar year will focus on the R&D of a second APEX prototype in a ton-scale TPC at CERN and/or Fermilab. The prototype will reflect the actual APEX panel geometry on smaller dimensions primarily for mechanical and cryogenic tests. A PD module prototype with a full electronic chain, including PoF and SoF systems, will be realized and tested in parallel before being integrated into the ton-scale TPC prototype. A larger-sized APEX demonstrator in a several cubic meters LAr cryostat, with O(100) SoF and PoF in/out fibers will be a third stage prototyping goal in 2024-25. The DUNE cryogenic lab at the Fermilab IERC building where a large 2m × 2m × 3m ColdBox facility for LAr technology development is being built will be ideal for these R&D steps. The last prototyping phase, with the deployment of a full-sized APEX PD-instrumented field cage in the VD protoDUNE cryostat at CERN for a 1-kT scale validation, will be pursued along with the proposed ARIADNE optical readout TPC program (Section 3.2.6).

The field cage, an element of the TPC HV System, as part of APEX has been designed to be compatible with any VD LArTPC solution for charge readout considered for the Phase II FD modules, with the PD integrated system offering a maximal optical coverage solution for light readout. VD LArTPC solutions with light readout integrated at the anode charge readout plane are also compatible and complementary, toward an ideal 4π coverage enhancing the light

yield of the combined light system near the anode planes.

3.2.2 Strip-based charge readout on anode (Dominique, Dario, Cheng-Ju)

FD2-like some notes:

- alternate and simpler methods to connect the various views
- optimization of strip length vs. channel count
- optimization of strip pitch vs channel count
- Optimizations of the Bottom Drift Electronics (BDE) include options to port the LArASIC, a custom pre-amplifier and shaping ASIC, from 180 nm to 65 nm process. This is to mitigate the risk of losing access to the 180 nm production line. The two other custom ASICs, ColdADC and COLDATA, are already using the 65 nm production process. Another improvement for the BDE design is to optimize the signal and power distribution scheme to potentially reduce the cable length needed (27 m for the current FD2 design) and simplify the far detector installation.
- other...

3.2.3 Pixel-based charge readout on anode (Joanathan, Dan)

Pixel-based readout replaces the multi-layer strip-based readout with a single-layer grid of charge-sensitive pixels at mm-scale granularity. By instrumenting each pixel with a dedicated electronics channel, a LArTPC with true and unambiguous 3D readout is achieved. Given channel densities of $O(10^5)$ pixels per m^2 of anode, pixel readout must operate at O(100) μW per channel in order to avoid excessive heating of the LArTPC detector. Recent years have shown significant progress in the development of pixel readout for LArTPCs, overcoming issues with excessive waste heat, as well as demonstrating cryo-compatibility, $O(10^4)$ digital multiplexing, and cost-effective scalable production.

3.2.4 LArPix

LArPix is a complete pixel readout system for LArTPCs, consisting of 6400-channel pixel anode tiles, cryogenic-compatible data and power cabling, and a multi-tile digital controller with an integrated operating system. It has been developed as the baseline technology of the DUNE Liquid Argon Near Detector (ND-LAr). The system relies on the LArPix application-specific integrated circuit (ASIC), a 64-channel detector system-on-a-chip that includes analog amplification, self-triggering, digitization, digital multiplexing, and a configuration controller. The LArPix-v1 ASIC demonstrated that waste heat could be controlled through a custom low-power amplifier and channel self-triggering, where the digitization and digital readout are dormant until a signal is detected on the pixel. The LArPix-v2 ASIC incorporated a variety of improvements to facilitate large-scale production of pixel anodes, including Hydra-IO, a novel

Figure 12: Prototype LArPix-v2 anode tile 32 cm in length by 32 cm in height with 6400 gold-plated charge sensitive pixel pads at 3.8 mm pitch (left) driven by 100 LArPix-v2 ASICs (right).

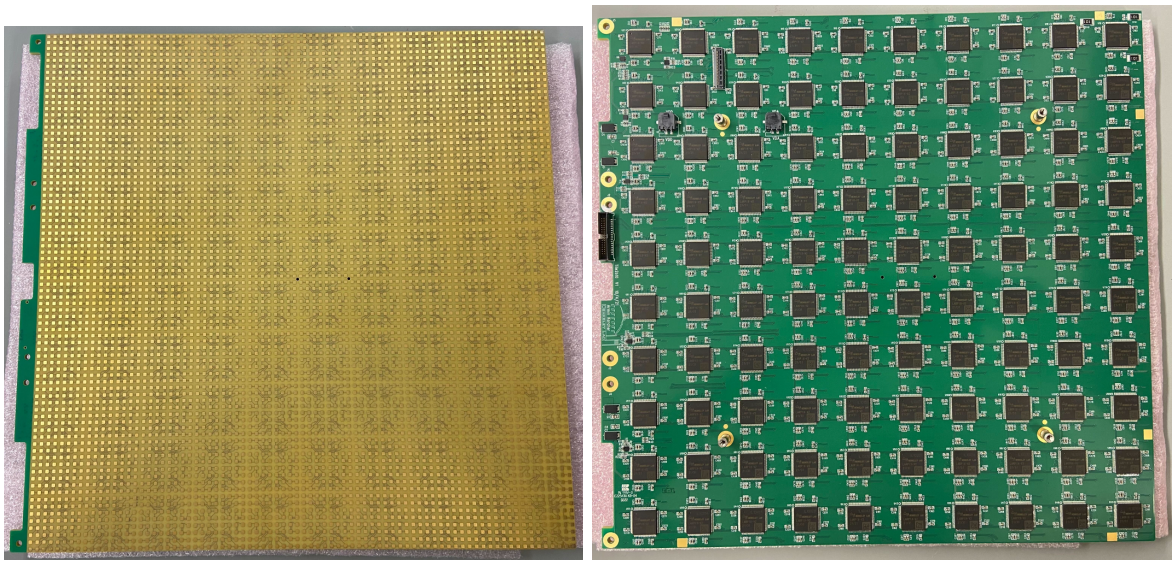

programmable chip-to-chip data routing technique to improve system reliability in the inaccessible cryogenic detector environment. The current 32 cm by 32 cm LArPix pixel tile (see Fig. 12) has 6400 charge-sensitive pixels at 3.8 mm pitch and can be configured and read out via a single set of differential digital input and output wires. The design leverages standard commercial techniques for printed-circuit board (PCB) production to realize a LArTPC anode, achieving 800 e^- equivalent noise charge on the sensitive TPC-facing side, while powering and communicating with 100 LArPix ASICs on the tile back side. The tile control electronics (a.k.a. PACMAN) are responsible for delivering power and communication to the tiles, and a single compact controller is currently capable of driving O(10) pixel tiles (e.g. O(10^5) pixels). It includes a CPU with integrated operating system and programmable logic similar to a field-programmable gate array (FPGA). The controller is designed to mount on the room-temperature side of a LArTPC cryostat feedthrough, and incorporates power filtering and ground isolation to ensure the integrity of the low-noise environment within the detector.

Approximately 80 LArPix-v2 pixel tiles have been produced as part of the current prototyping program for the DUNE Near Detector. Sets of 16 pixel tiles have been used to instrument each of the four LArTPC modules of the 2x2 Demonstrator (Fig. 13), a prototype of the modular LArTPC design planned for the Near Detector. Each ton-scale module has been operated at the Univ. of Bern, and have been used to image over 100 million cosmic ray events.

The LArPix-v2 development program has achieved its goal of a *scalable* design. All components are produced via commercial vendors using traditional electronics production techniques, and are ready for integrated testing; no additional assembly is required. LArPix-v2 system production costs, including all cabling, controllers, and power supplies, are approximately $10k per square meter.

Figure 13: A photograph of one of the four ton-scale LArTPC modules for the 2x2 Demonstrator, a prototype of the DUNE Near Detector (left), and an example cosmic ray imaged in true 3D using a 102,400-channel LArPix-v2 system in this module (right).

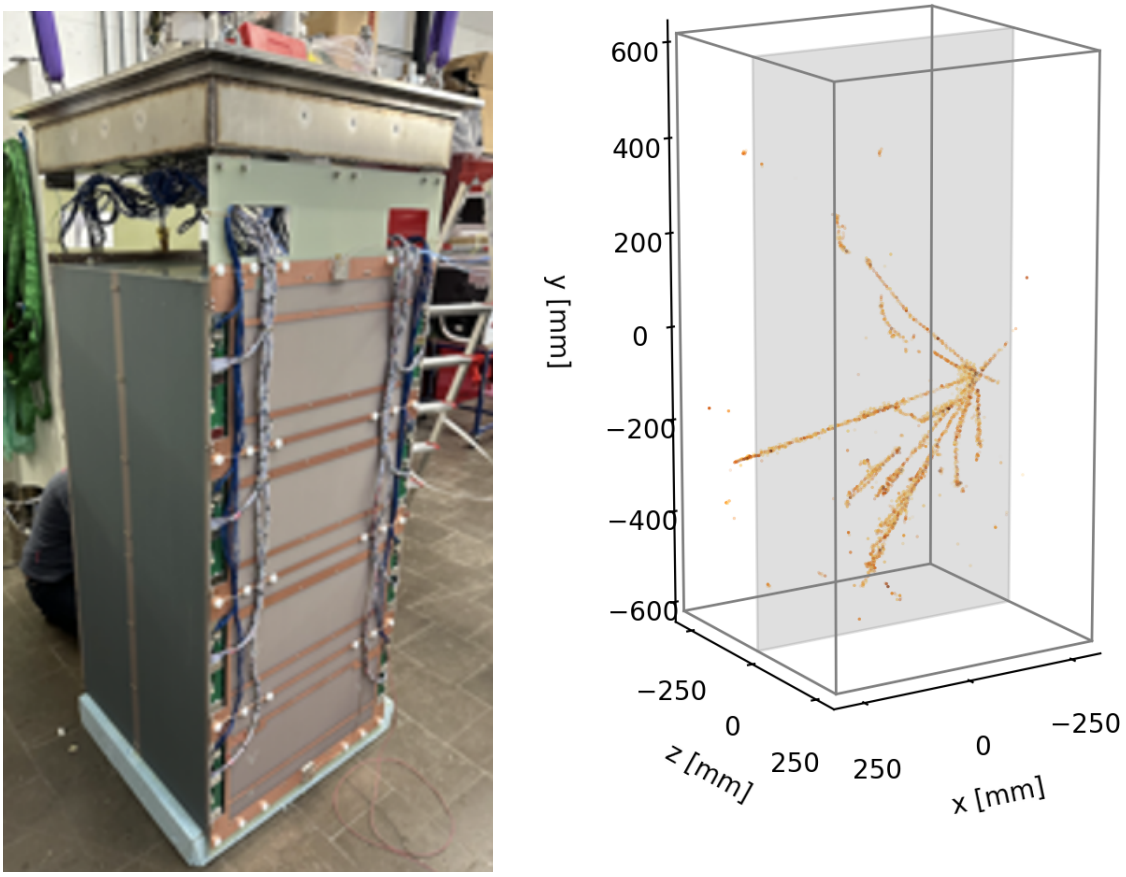

Assuming completion of the development program of LArPix for the DUNE Near Detector, LArPix would already meet most of the requirements for deployment in a future Far Detector module. The development and integration of a high-speed, O(1) GHz, 16-to-1 digital multiplexer would significantly reduce the cable plant, making deployment in a far detector much more feasible. Tests of a large-scale LArPix prototype in ProtoDUNE-VD system at the CERN Neutrino Platform are important to validate the integration and interfaces with the other aspects of the VD design.

A variant of LArPix has been designed for scalable readout of very large arrays of silicon photomultiplers (SiPMs). Called LightPix, this ASIC reuses much of the LArPix system design to provide a system that can read out $>10^5$ SiPMs in a cryogenic environment at costs of $\ll$\$1 per channel. A prototype LightPix system has been used in combination with VUV-sensitive SiPMs to detect cosmic rays in LAr. LightPix may be useful for instrumenting a future far detector with higher quantities of SiPMs than the current design.

3.2.5 Q-Pix

The basic concepts of the Q-Pix circuit are shown in Fig. 14 (A). The input pixel, labeled as "In," is envisioned to be a simple circular trace connected to the Q-Pix circuit by a via in a printed circuit board. The circuit begins with the "Charge-Integrate/Reset" (CIR) circuit. This charge-sensitive amplifier continuously integrates incoming signals on a feedback capacitor until a threshold on a Schmitt trigger (regenerative comparator) is met. When this threshold is met, the Schmitt trigger starts a rapid "reset" enabled by a MOSFET switch which drains the feedback capacitor and returns the circuit to a stable baseline and the cycle is free to begin again.

In order mitigate any potential charge loss which can occur during a reset and to allow for the CIR circuit to keep up with arbitrarily large charge deposits, an alternative design known as the "replenishment" scheme has also been evaluated. In contrast to the reset architecture, the MOSFET now functions as a controlled current source such that when the Schmitt trigger undergoes a transition, the MOSFET replenishes a charge of $\Delta Q = I \cdot \Delta t$, where Δt is the reset pulse width or discharge time. This ΔQ then forms a charge quantum of each transition. Even if there is a significant input charge during the discharging process, as long as the MOSFET current and the discharge time are fixed, the quantization ΔQ of each measurement will remain constant. This allows the Q-Pix to discharge the C_f through the MOSFET and integrate with the input current simultaneously without loss of charge.

This "reset/replenishment" transition pulse is used to capture and store the present time of a local clock within one ASIC (application-specific integrated circuit). This changes the basic quantum of information for each pixel from the traditional "charge per unit of time" data format to the difference between one clock capture and the next sequential capture, referred to as the "Reset Time Difference" (RTD). This new unit of information measures the time to integrate a pre-defined charge (ΔQ). Physics signals will produce a sequence of short [$\mathcal{O}(\mu s)$] RTDs. In the absence of a signal, the quiescent input current from backgrounds (^{39}Ar), cosmogenic, and other radioactivity) would be small and the expected RTDs are on the order of seconds.

Signal waveforms can be reconstructed from RTDs by exploiting the fact that the average

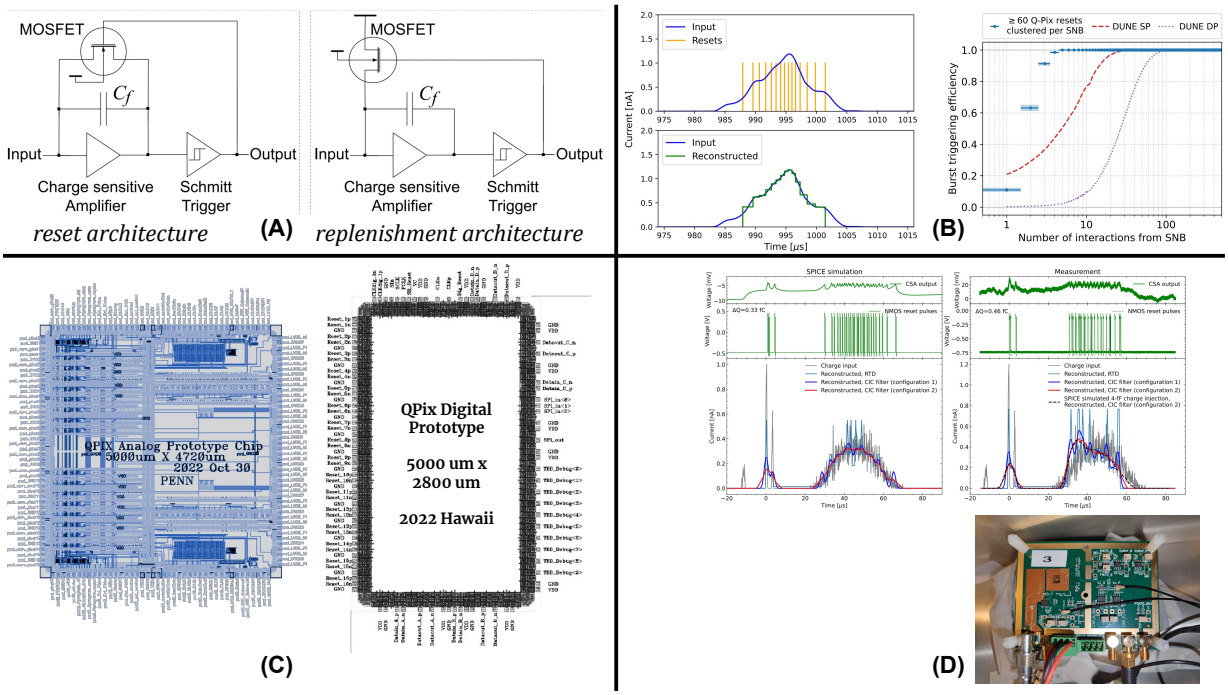

Figure 14: Add caption about Q-Pix.

input current and the RTD are inversely correlated ($I \propto 1/\text{RTD}$), where I is the average current over an interval ΔT and thus $I \cdot \Delta T = \int I(t)\,\mathrm{d}t = \Delta Q$. The signal current is captured with fixed ΔQ, determined by the charge integrator/reset circuit, but with varying time intervals. This architecture of Q-Pix makes the time at which a reset occurs the fundamental quanta of information.

Q-Pix has shown that this architecture can enhance the physics capabilities of a large scale LArTPC's through its ability to have low-threshold, high granularity readout. The first of these demonstrations shows the improved reconstruction enabled by a pixel based detector when compared to a projective based readout for multi-GeV neutrino interactions (such as those which would be seen in future long-baseline experiments like the Deep Underground Neutrino Experiment) [**?**]. This analysis showed enhanced effiency and purity across all neutrino interaction types analyzed and the ability to reconstruct the topology and content of the hadronic topology (including number of final state protons, charged, and neutral pions). Moreover, through an analysis of supernova neutrino interactions and a simulation of the Q-Pix architecture it was shown that Q-Pix can signficantly enhance the low energy neutrino capabilities for kiloton scale LArTPC's. Specifically, Q-Pix enhances: i) enhances the efficiency of reconstructing low energy supernova neutrino events over the nominal wire based readout, ii) allows for a high purity and high efficiency identification of supernova neutrino candidates, iii) affords these enhancements at data rates 10^6 times less for the same energy threshold, and iv) allows for supernova burst pointing accuracy to < 20 degrees from a single 10kTon module.

A number of prototypes are currently under construction and evaluation to demonstrate the Q-Pix readout architecture. These include designs in both CMOS 180 nm and 130 nm,

evaluation of the architecture using discrete commercial-off-the-shelf components (COTS), as well as extensive digital prototyping using field programmable gate arrays (FPGA's).

The 130 nm design implements the basic "reset" architecture via a simple analog integrator (xx mv/fC), comparator, and NMOS reset transistor. This design was done in the open-source Skywater package and was not optimized for power consumption with instead its design focused on demonstrating the functionality and thus is estimated to consume $\sim 75 - 150\mu$W/channel. The 180 nm design consists of a 16 channel analog chip with the replenishment architecture implemented and a 16 channel digital chip and was optimized to lower the power consumption of the chip. The analog chip contains 8 "Standard" gain channels and 8 "C-gain" (capacitor based gain) channels. Each bank of 8 channels has its own services inculding serial interface, ring oscillator, POR (Power-On Reset), and calibration circuit. "Standard" gain channels consist of an analog Integrator (20mv/fC), an intermediate amplifier (x3), comparator and programmable replenishment circuitry and is estimated to consume $\sim 45\mu$W/channel. "C-gain" channels have the same functionality but use a different analog Integrator with much higher gain (48mv/fC) to avoid the need for an intermediate amplifier. This reduces unknown offsets, reduces internal delay and power and allows a wider range of bandwidth vs intrinsic noise tradeoffs. The "C-gain" channels have a power consumption estimated to be $\sim 25\mu$W/channel. The digital chip contains 16 differential inputs, digital memory (local and global buffers), ring oscillator and implements the "ENDEVOUR" readout protocol with LVDS output. The layout of the chip is shown schematically in Figure 14 (C).

Figure 14 (D) shows the implementation of replenishment architecture for the Q-Pix readout done using COTS discrete components. This prototype was able to demonstrate the fidelity of reconstructing input from an arbitrary wave-form generator with a replenishment threshold of 0.46 fC with replenishment pulse widths $\sim 300 - 600$ ns and linear responses to replenishment up to 2 MHz rates. This demonstration provides confidence that the architecture proposed will be capable of meeting the performance needs of future large scale LArTPC's. The consortium of universities and labs working on this project expect both small and large scale demonstrations ($\mathcal{O}(1000 - 100,000)$ pixel) LArTPC's in the coming next few years.

3.2.6 Optical-based charge readout on anode (Kostas, ARIADNE-like)

The optical charge readout with fast cameras was developed within the ARIADNE program and represents a cost-effective and powerful alternative approach to the existing charge readout methodology. As first demonstrated in the 1-ton dual-phase ARIADNE detector, the secondary scintillation (S2) light produced in THGEM holes can be captured by fast TimePIX3 cameras to reconstruct in 3D the primary ionisation track.

The operation principle of a dual phase optical TPC read out with a TimePIX3 system is shown in Figure 15a. When a charged particle enters the LAr volume it causes prompt scintillation light (S1) and ionisation. The free ionisation electrons are drifted in a uniform electric field to the surface of the liquid. A higher field induced between an extraction grid and the bottom electrode of the THGEM extracts the electrons to the gas phase. Once in gas, the electrons are accelerated within the 500 μm holes of the THGEM at a field set between 22-31 kV/cm. As well as charge amplification, secondary scintillation (S2) VUV light is produced.

Figure 15: a) Detection principle of dual phase optical TPC readout with TimePIX3 camera, first demonstrated in the 1-ton ARIADNE detector. b) LAr interactions from cosmics. Figures taken from [24].

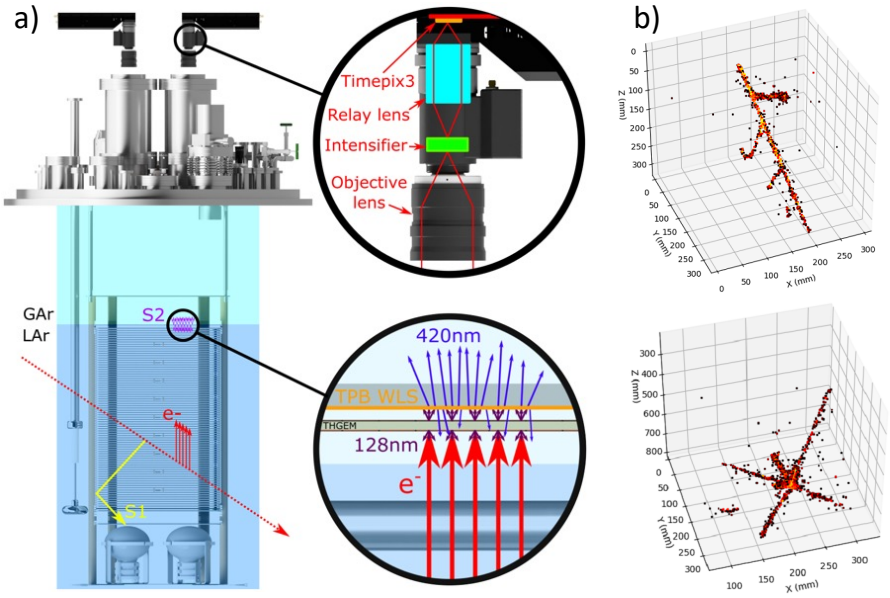

The light is shifted with a TPB coated sheet to 430 nm and then detected by cameras mounted on optical viewports above the THGEM plane.

Originally optical readout was tested with EMCCD cameras within the 1-ton ARIADNE detector at the T9 charged particle beamline at CERN [25] and later was upgraded with fast TimePIX3. Within the TimePIX3 camera assembly, a lens coupled to a Photonis Cricket image intensifier (33% quantum efficiency at 430 nm) boosts the S2 light signal. The amplified photons hit light sensitive silicon, bump bonded to a TimePIX3 chip (55 μm, 256 $\times$ 256 pixel array). The camera measures simultaneously 10-bit Time over Threshold (ToT) and Time of Arrival (ToA); ToT allows accurate calorimetry and ToA gives accurate timing (1.6 ns resolution). The TimePIX3 chip then sends a packet containing 4 pieces of information: x and y pixel position, ToA (z) and ToT allowing for full 3D reconstruction using a single device. The camera provides a "Data driven readout" where pixels are read out asynchronously allowing for very efficient sparse readout; the maximum readout rate is 80 Mhits/s. The high readout rate, natively 3D raw data and low storage due to zero suppression make TimePIX3 ideal for optical TPC readout.

The TPX3 camera system was first tested in low pressure CF4 gas within the ARIADNE 40 l TPC prototype [26]; following this demonstration, a TimePIX3 camera was mounted on ARIADNE and particle tracks from cosmic showers were successfully imaged in 3D for first time (see Figure 15b) [24]. The cameras are shown to be sensitive even to pure electroluminescence light generated at the lower end of the THGEM field; this mitigates difficulties often faced when trying to operate THGEMs at a higher field where there can be issues with stability. Use of cameras has additional benefits such as ease of upgrade as they are externally mounted, they

are decoupled from TPC and acoustic noise and as, large areas can be covered with one camera bringing cost and operational benefits.

Figure 16: a) The LRP under the cryostat lid. b) The ARIADNE$^+$ team on top of the cryostat. c)A LAr interaction.

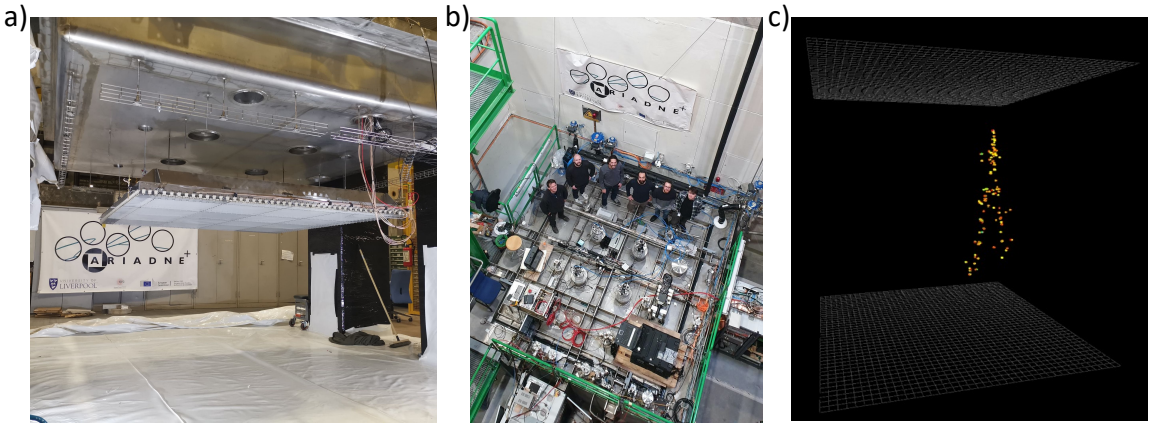

In order to demonstrate this technology further and at a scale relevant to the 10 kton DUNE detector modules, a larger-scale test (ARIADNE$^+$) was proposed [27] and recently performed at the CERN Neutrino Platform. Four cameras, each imaging a 1m $\times$ 1m field of view were employed of which one utilised a novel VUV image intensifier negating the need for wavelength shifter. The test also showcased a light readout plane (LRP) comprising of 16, 50 $\times$ 50 cm glass THGEMs supported within an Invar welded structure. The novel manufacturing process for the glass THGEMs allows for mass production at the large-scale [28]. Successful, stable operation was achieved, and cosmic muon data were collected from both the visible and VUV intensifiers showcasing optical readout technology in combination with a novel glass THGEM array. An image of the detector setup is shown in Figure 16 and results are published in [29]. Further R&D into custom optics and characterisation of the next generation TPX4 cameras is foreseen. A proposal to the CERN SPSC to instrument the ProtoDUNE NP02 cryostat with optical readout is underway.

3.2.7 Integrated charge and light readout on anode (Stefan, Jonathan)

This is still cut and paste from another document and needs adjustements.

The SoLAr technology will be based on the concept of monolithic light-charge pixel-based readout which has a low energy threshold with excellent energy resolution ($\approx$ 7%) and background rejection through pulse-shape discrimination.

The SoLAr readout unit (SRU) is a pixel tile based on PCB technology that embeds charge readout pads located at the focal point of the LArTPC field shaping system and collects drifting charges, and VUV SiPMs to collect photons in thousands of microcells operated in Geiger mode. In order to maintain a uniform electric field, new novel monolithic VUV SiPM sensors need to be developed that have charge readout pads and highly efficient UV-light sensitive microcells.

In 2020, a joint research program between liquid-argon detector scientists and one of our industrial partners (Hamamatsu Photonics) delivered a Silicon Photomultiplier (SiPM) that reached a record efficiency (15% PDE) for 128 nm light at the argon boiling point (87K). Nearly at the same time, the first integrated system for multiplexing the SiPM signal was commissioned and operated inside strong electric fields. In 2021 a further development with Hamamatsu Photonics produced new SiPMs with through silicon vias that will enable the combination with the charge readout required for SoLAr.

In the SoLAr preparatory phase (2021-2022) [Navrer-Agasson2022], we demonstrated combined light-charge collection using small-size prototypes at Bern. The prototype was operated successfully and has demonstrated that the envisaged principle of combining charge and light readout is possible (Fig. 1). Simulations have shown that a 7% resolution can be achieved by replacing anode planes with a pixelated readout integrating a light-sensitive area covering 10% of the surface. This system enhances the amount of collected light by a factor of 5 compared with the first DUNE module. The authors of Ref. [Capozzi2019b] have studied the remarkable impact of energy resolution in the background budget of a LArTPC with conventional readout in a membrane cryostat.

The combination of shielding and a 7% energy resolution gives access to the 5-10 MeV region - where most of 8B neutrinos reside - by removing the dominant background from neutrons and 42K down to 5 MeV and 39Ar down to 1 MeV. The energy resolution is instrumental to sharpen the 17 MeV cutoff of the 8B neutrino spectrum, which lies just below the hep cutoff of 18.8 MeV, and opens a 1.8 MeV window to observe a pure sample of hep neutrinos [Kubodera2004] Light collection outside the anode is ensured by conventional X-ARAPUCA tiles located outside the field-cage for a total coverage of $8-10\%$. The latter provide the appropriate light yield without resorting to xenon doping, thus preserving the pulse-shape discrimination power of liquid argon. Pulse shape discrimination is further enhanced with respect to any existing LArTPC by the unique performance of the SRU and the increase of collected light.

Finally, SoLAr will deliver a novel membrane-based cryogenic system that provides both neutron shielding and a radiopure environment to suppress environmental background to the limit where the only residual background is generated inside the LArTPC. SoLAr will demonstrate neutron shielding embedded directly in the cryostat walls and reduce external neutron background in the 1-4 MeV region by three orders of magnitude.

Q-Pix is also pursuing integration of both light and charge detection modes on the anode into a single integrated detector element. If such a device could be made sensitive to both UV photons directly as well as light at other wavelengths at reasonable quantum efficiency this would revamp the way noble element detectors attempt to utilize both the charge and light signals. Such a new detector element would offer: i) the intrinsic fine grain information for both the charge and light opening up new exciting possibilities to exploit the imaging capabilities for both signals, ii) monumentally enhance the amount of light collected near the anode through increased surface area coverage, and iii) simplification in the design and operation of noble element detectors.

One such method considered is coating a pixel based charge readout with a type of photoconductive material that when struck by a UV photon would generate a signal (charge) which could be detected by the same charge readout scheme considered for the ionization charge. This

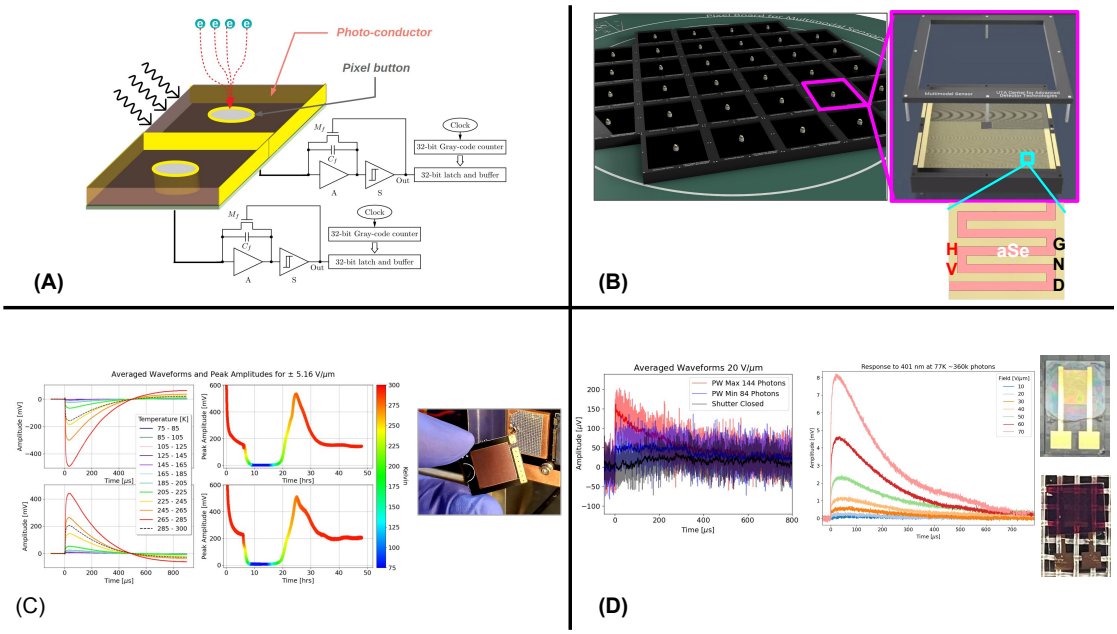

Figure 17: Add caption about Q-Pix Light.

idea is shown schematically in Figure 17 (A). Moreover, with the proper choice of photoconductor such a device could have a broad frequency response and thus all the detection of the full spectrum of light produced in noble element TPCs.

Three such photoconductive materials have been explored initially in recent R&D: i) amorphous selenium (aSe), ii) zinc oxide (ZnO), and organic photodiodes (OPDs) and their application in a liquid argon environment is currently under investigation. Initial studies of constructing a multimodal pixel detector have recently focused on utilizing aSe as the ability to prototype and test was the simplest. Designs for a multimodal pixel are shown in Figure 17 (B) where an interdigitated electrode (IDE) is deposited around the central ionization collection pixel. This design provides a straightforward way to incorporate the ability to apply a local electric field to the aSe an enable charge gain as well as instrument the area between the charge collection pixels. Figure 17 (c) shows the first study of this design, done at small scale on commercially manufactured PCB's [**?**]. This study showed the viability of an IDE based aSe device at cryogenic temperatures with a response to VUV photons. More recent studies have pushed this capability further to characterize the performance of such a design to a low photon

flux ($\mathcal{O}(100)$ photons and at high electric fields ($> 70\text{V}/\mu\text{m}$) and at cryogenic temperatures. These results continue to show promise and further R&D into aSe based devices (as well as other photoconductors) is anticipated to be an area of active research in the near term future.

3.2.8 DAQ upgrade options for readout of vertical drift (Giovanna)

(enhancements in computing technologies, machine learning at early stages of DAQ)

3.3 Background control (Chris, Eric)

The potential to enhance the physics scope of DUNE phase 2 with lower energy thresholds has been attracting significant attention within the wider community [refs]. All these ideas tend to rely on two enhancements over the Phase 1 program: greater control of radioactive backgrounds and improved energy resolution at lower energies. DUNE is well placed to improve the lower energy physics scope due to the depth of the far detector which is well shielded from cosmic induced backgrounds, and the sheer size of the argon volume which allows significant fiducialization to reduce external backgrounds. Phase 2 designs which minimize material in the liquid argon target, such as the single-phase vertical drift or dual phase designs, are most favorable for low background physics due to reduced radioactive background risk.

The intrinsic backgrounds in the argon set two natural physics target regions. The first background target extends the threshold down to 5 MeV, just above the ^{42}K beta endpoint. With careful control of neutron, gamma, and radon related backgrounds, combined with improvements in the low energy readout of charge and light, an extended supernova burst neutrino programs can be envisaged, with improved reach in terms of supernova distance sensitivity (to the Magellan clouds), for elastic scatters with improved directionality, and to the softer energy early or late parts of the supernova spectrum. A low energy threshold could also allow a solar neutrino program with sensitivity to precision measurements to explore solar-reactor oscillation tensions and non-standard interactions. This 5 MeV threshold is set by the intrinsic ^{42}Ar-^{42}K decay chain and to go lower (background target 2) this intrinsic ^{42}Ar must be removed by using underground sources of argon. Below this threshold ambitious but high reward physics measurements include solar CNO measurements; searches for neutrinoless double beta decay with xenon loading; and even high mass weakly interacting massive particle dark matter detection could be possible [ref].

In this section we outline some of the most significant radioactive backgrounds and identify paths to reduce them in phase 2.

3.3.1 External Neutrons and Gammas

In DUNE phase 1 the dominant background to low energy supernova burst neutrinos will be from neutrons arriving from outside the detector, originating within the SURF cavern rock and shotcrete. These neutrons when they capture in the liquid argon can produce 6.1 MeV or 8.8 MeV gamma cascades which Compton scatter or pair produce electrons that directly mimic the charged current neutrino signals. To remove external neutrons passive shielding can be deployed, as first suggested in [ref]. 40 cm of water is sufficient to attenuate the

neutron flux from spontaneous fission or (alpha, n) in the rock by 3 orders of magnitude, making it subdominant. Such a shield is of the size to fit within the warm support structure of the cryostat. Alternative approaches would involve modifications to the cryostat design, for example layering or doping the insulating foam with neutron capturing materials such as boron, lithium, or gadolinium. These same measures will ameliorate the cavern gamma background originating from ^{238}U and ^{232}Th chains, and which without them will likely be high.

3.3.2 Internal backgrounds

After the external cavern neutrons, the most significant source of neutron background comes from detector materials, from (alpha, n) induced reactions within the cryostat and other components. Gammas produced in these events can also distort reconstruction algorithms due to flash or blip backgrounds, particularly when close to the readout such as the cryostat mounted light sensors. Dark matter experiments have successfully managed such backgrounds with careful material selection programs, using radioactivity assay to select favorable materials for detector construction and to ensure quality assurance during production and installation processes. The world leading dark matter detectors have lowered backgrounds by 5 orders of magnitude below the DUNE phase 1 target. To maintain the sub-dominance of these backgrounds relative to externals removed by shielding, DUNE phase 2 will require a less stringent three orders of magnitude reduction target.

3.3.3 Radon

Radon is highly mobile, emanates from all detector materials, and can diffuse easily throughout the whole argon target. This background can either mimic directly low energy neutrinos, through (alpha, gamma) interactions or mis-identified alpha events in the argon, or, can produce daughter products which can plateout on internal components such as the photon detector system and distort the low energy reconstruction. Several approaches should be adopted to control this background including: direct removal of radon in the purification system using an inline radon trap; selection of detector materials for low radon emanation in cryogenic liquid argon; surface treatments to contain or remove radon sources; removal of a significant emanation source from dust by controlling and cleaning to higher cleanliness standards than in Phase 1; removal of radon from air during installation to lower the risk of plateout backgrounds when the detector is open; and analysis techniques such as alpha tagging by pulse shape discrimination.

3.3.4 Intrinsic Argon Backgrounds

Argon extracted from the atmosphere contains two background isotopes that can limit sensitivity at the lowest energy: ^{39}Ar, with a decay Q-value of 565 keV; and ^{42}Ar with a decay Q-value of 599 keV and a daughter isotope of ^{42}K which decays with a Q-value of 3525 keV. The ^{42}Ar-^{42}K chain sets a lower limit of about 5 MeV (dependent on the ultimate low energy resolution) for low threshold physics with atmospheric argon. Dark matter experiments have successfully extracted argon from underground sources which are depleted in both ^{42}Ar and ^{39}Ar [ref]. These experiments show reduction factors of order 1400 for ^{39}Ar and have seen no

^{42}Ar. The currently only known source of underground argon is too small to fill a detector the scale of DUNE, but work is ongoing to identify new, larger sources which can be used cost-effectively. Recent estimates of the potential reduction of ^{42}Ar in underground sourced argon is expected to be 8 orders of magnitude [ref].

3.3.5 SLoMo

One proposed design for a low background phase 2 far detector is the SURF Low Background Module, SLoMo. This design provides a path to lower background levels using the techniques outlined above, reducing most backgrounds sources by three orders of magnitude below the expected phase 1 levels. This is combined with a significant increase in light coverage within the detector using high quantum efficiency DarkSide-style SiPM tiles [ref] to increase the energy resolution and pulse shape discrimination power at lower energies.

To get this light coverage, SLoMo aims to densely instrument an interior 1-2 kTons of highly fiducialized underground argon (UAr) in the center of a VD-like detector. The structure on which to mount the DarkSide SiPM modules is not fixed in this design, though we propose light-tight acrylic walls covered in wavelength-shifting foils. We show [ref] that a 20% SiPM coverage, combined with charge detection by existing VD CRPs, viewing an interior volume should easily lead to a sub-2% energy resolution at 2 MeV. This feature, along with the negligibly low amount of ^{42}Ar in UAr, makes possible $0\nu\beta\beta$ studies with Xe loading, should this be a program DUNE wishes to pursue. Reducing ^{42}Ar to very low levels also allows supernovae visible neutrino energy spectra to reach well down into the region where $\nu_e e$ elastic scattering dominates and thus pointing, in principle, is improved. We observe that 20% SiPM module coverage comes at an affordable cost and counts enough photons to allow pulse shape discrimination, so that along with the combination of low neutron background, fiducialization and radon controls, SLoMo enables a competitive WIMP dark matter search. We show, as well, that solar CNO investigations become possible, for example, as does observation of further phenomena, such as the supernovae "glow" [ref].

This design is outlined in reference [ref] where the significant physics gains are further explicated.

3.3.6 R&D needs

All the Phase 2 options to lower the energy threshold require a radioactive background budget to be specified and low background techniques to be deployed to ensure it is achieved. The research and development required to achieve these goals includes:

- Compact shield designs, that can fit in the limited DUNE cavern space or within the cryostat structure.
- Large-scale materials & assay campaigns, scaling up material selection techniques used by low background fundamental physics experiments from the few-ton-scale to the kton-scale.
- Cleanliness requirements and approaches for the kton scale.

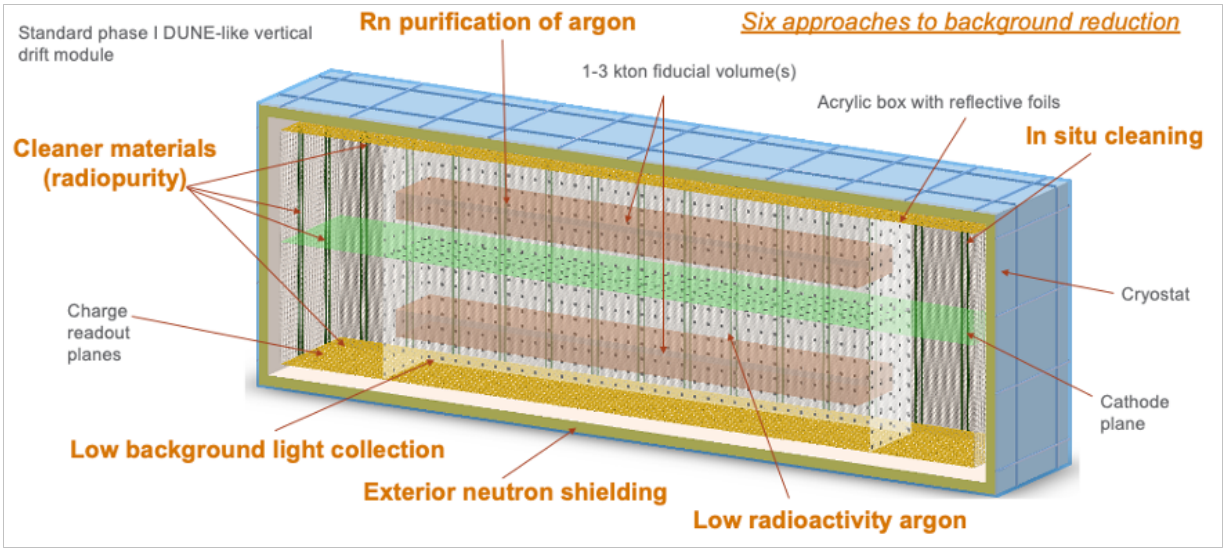

Figure 18: Design for SLoMo, highlighting background control methods required to achieve goals.

- Radon control in noble liquids, including emanation assay and control at DUNE-scale.
- New sources of underground argon, capable of filling a DUNE module cost-effectively.
- Low background photon detection systems, developing new designs that can increase the light detection efficiency without overwhelming a background budget.
- Background model and simulation campaign for physics sensitivity analyses
- Novel analysis techniques, such as pulse shape discrimination, to remove background events.

3.4 Xe-doped LAr (Andy)

A promising direction for expanding DUNE capabilities in a Phase II far detector module is to introduce dopants to the liquid argon, creating a target other than pure liquid argon. Generically, these LAr "doping" techniques may be used to modify the detector response in a desirable way or to introduce new materials of interest into the bulk detector volume. These approaches are analogous to widely-used strategies in e.g. scintillator or solid state detectors, where for example secondary fluors are added to scintillators to shift photon wavelengths, or elements like gadolinium or lithium are added to increase neutron or neutrino cross sections, respectively. A key constraint for LAr dopants is that they must not interfere with the operation of the LArTPC by introducing electronegative impurities that non-negligibly degrade the LAr transparency to electrons. Furthermore, as for any large-scale detector with complex physics of signal generation, the relevant microphysics (including radiative and non-radiative molecular

energy transfer, electron-ion recombination, and scintillation light production) must be well-understood through a robust R&D program to adequately assess the scalability to the DUNE FD scale. Several such avenues are being explored that would enhance the charge or light detection capabilities or introduce new signals of interest. In this section, we will consider two promising potential additives that have been previously demonstrated in large-scale LArTPCs. The first category includes photosensitive dopants that convert scintillation light to ionization charge. The second is liquid xenon, which is of interest at low concentrations for impact on the scintillation light signal, and at higher concentrations as a signal source.

These LAr dopants can be particularly impactful for the prospects for DUNE Phase II to broaden the low-energy physics program, targeting signals in the MeV to keV energy range. Detection of signals in this regime can both enhance the GeV-scale neutrino oscillation physics program through enhanced neutrino energy reconstruction [30], but also provide sensitivity to a broad array of previously inaccessible signals spanning Beyond the Standard Model physics and low-energy neutrino astrophysics. Examples include low-energy solar and supernova neutrinos, searches for rare decays such as neutrinoless double-beta decay, exotic physics such as fractionally-charged particles, and dark matter scattering. A more complete list can be found in Ref. [31]. An expanded program in these areas would complement DUNE's program while leveraging the large mass and deep-underground location.

Photosensitive dopants In a typical pure-LAr TPC, the energy deposited by charged particles is ultimately divided between ionization electrons drifted in the TPC electric field and detected at the anode plane and scintillation light detected by a photon detection system. The light signal, which is produced promptly with ns-scale timing, is used for 3D event position reconstruction as well as triggering and absolute timing of neutrino interactions. In a LArTPC doped with a photosensitive dopant, the scintillation signal would be converted to ionization charge, effectively transferring the full deposited energy into that channel. Potential photosensitive dopants under consideration are a class of hydrocarbons with work functions on the order of the LAr (or Xe-doped LAr) VUV primary scintillation photon energy (7–9 eV), which provide highly efficient conversion of scintillation light into ionization electrons with minimal loss to spatial resolution.

The use of such dopants in LArTPCs can offer benefits to both the GeV– and MeV-scale physics programs of DUNE Phase II. In general, the transfer of deposited energy into the ionization channel leads to an enhancement of the ionization charge, which is measured with excellent efficiency in a LArTPC. This enhancement is particularly pronounced in regions of high energy deposition, improving prospects for particle identification using charge calorimetry. Furthermore, LAr with photosensitive dopants exhibits a significantly more linear relationship between deposited and visible charge, reducing the scale and uncertainties of corrections related to electron-ion recombination effects. The general impact of such dopants in large-scale LArTPCs in practice has been studied previously: the ICARUS collaboration performed a long-term test of dopant tetramethyl germane (TMG) in a 3 ton LArTPC exposed to cosmic rays and gamma sources, observing a clear enhancement in the ionization charge signal, and a significantly more linear response in reconstructed to deposited charge [32]. Importantly, this test also demonstrated long-term stability in realistic LArTPC operating conditions. A

complete detailed model of the microphysics of energy transfer between LAr and candidate photosensitive dopants will require dedicated R&D, to provide a comprehensive assessment of potential dopants and their ionization response across a broad range of signal energies for the Phase II program.

The enhancements provided by photosensitive dopants are particularly notable for the low-energy physics program, considering pointlike signals at or below the MeV scale in energy. A significant challenge with measuring such signals is the efficient collection of small amounts of scintillation light. With only a fraction of the energy deposited by a particle through ionization of the liquid argon ultimately contributing to an ionization electron signal, the balance are emitted as scintillation photons which are detected with efficiency approximately at the percent level. In the Phase I design, a limited photon collection efficiency would limit the capabilities of DUNE to extract spectral information regarding MeV-scale signals, and relatedly to perform energy-based background mitigations. Ideally, a detector would measure both of these anticorrelated signals to measure a precise total energy, as in the case of the EXO-200 experiment [33] and also investigated in LArIAT [34]. In principle, a large LArTPC can achieve percent-level energy resolution for MeV-scale signals of interest, but this would require detection of tens of percent of the scintillation photons, a level of efficiency impractical with current and near-future designs. Meanwhile, by converting the isotropic scintillation light into directional ionization charge, photosensitive dopants at the ppm level could allow the full energy to be measured with high efficiency by the TPC charge detection system. In this sense, charge alone would provide a precise energy measurement, analogous to a correlated charge/light measurement. Previous work in the context of LAr calorimeters has also considered the impact of several candidate dopants on MeV-scale alphas, demonstrating substantial change enhancements for low-energy events with relatively large scintillation signals [35]. Straightforward future R&D using beta or gamma sources to study the low-energy electromagnetic response can further clarify the impact and achievable energy resolution for MeV-scale signals of interest for neutrino energy measurement, low-energy neutrino astrophysics, and keV– to MeV-scale BSM signatures.

Photosensitive dopants could afford benefits to event reconstruction, particle identification, and allow for lower thresholds across a Phase II program. Taken together, past R&D work has clearly demonstrated the expected enhancement of the ionization charge signal, and also illustrated the potential gains for low-energy signal reconstruction and energy resolution at the MeV scale. To fully realize the potential will require further studies, to explore the microphysics involved, establish the achievable energy resolution with MeV-scale electrons, and determine the optimal dopant types and concentrations to maximally benefit the MeV– and GeV-scale physics programs in DUNE Phase II.

Liquid xenon Liquid xenon is a second potential additive to the LAr in DUNE Phase II, either at a low (ppm) or high (up to percent level) concentration. The loading techniques [36] and stability conditions [37] of LAr+LXe mixtures have been explored across this broad range of concentrations.

At low concentrations, the presence of Xe impacts the production of scintillation light in LAr, acting as a highly efficient wavelength shifter converting the 128 nm primary scintillation

wavelength in argon to a longer 178 nm wavelength. This has several advantages, including improved uniformity due to reduced Rayleigh scattering, a narrowing of the scintillation timing distribution, and relatedly, a dramatic reduction in energy losses to impurities such as nitrogen that would result from non-radiative energy transfers involving the long-lived triplet state of Ar that is suppressed with the introduction of Xe. This leads to much improved robustness of the scintillation light yield against LAr impurities, without appreciable impact on the charge signal. Xe doping up to $\sim$ 20 ppm has been demonstrated with ProtoDUNE-SP, which verified the enhancements to optical response and the recovery of light yield in the presence of impurities using a 770 ton single-phase LArTPC functionally identical to the DUNE Phase I single-phase FD [36].

At higher concentrations, up to the percent level, Xe may also be of interest as a signal source. 136Xe is a candidate isotope for neutrinoless double-beta decay (NLDBD), which if observed would establish the Majorana nature of the neutrino and demonstrate a violation of lepton number conservation [38]. The introduction of Xe either in its natural form (8.9% 136Xe) or enriched in the NLDBD isotope into a large-scale, deep-underground LArTPC detector could provide an opportunity to search for this important decay mode [39]. Mitigation of important backgrounds (^{39}Ar, ^{42}Ar, neutrons) near the 2.5 MeV Q-value for this decay are consistent with the requirements of other potential low-energy physics goals considered for DUNE Phase II, as described in Section 3.3. A key challenge for a competitive search is achieving an energy resolution at the percent level for MeV-scale electrons; photosensitive dopants provide one avenue toward achieving this.

3.5 Water-based liquid scintillator (Theia) (Gabriel)

Theia is motivated by a rich program of low-energy astroparticle, rare event, and precision physics beyond the reach of the baseline LAr technology (Sec. 3.5.1), along with comparable CPV sensitivity to a baseline LAr-TPC module (Sec. 3.5.2). Theia leverages hybrid detection technology (Sec. 3.5.3) to offer enhanced particle and event identification at both low- and high-energy, coupled with a high radio-purity target, no inherent radio isotopes, and excellent neutron shielding. This allows the detector to probe physics that requires low threshold and low background, such as low-energy solar neutrinos, such as the CNO-cycle neutrino flux, and even neutrinoless double beta decay (NLDBD). The technology necessary for Theia is at an advanced stage, with several technology demonstrators under construction, with data expected in FY24 (Sec. 3.5.4).

3.5.1 Theia physics program

Theia, named for the Titan Goddess of light, seeks to make world-leading measurements over as broad range of neutrino physics and astrophysics as possible. The scientific program includes: observations of low- and high-energy solar neutrinos – both a precision measurement of the CNO flux, as well as a probe of the MSW transition region; determination of neutrino mass ordering and measurement of the neutrino CP-violating phase δ; observations of diffuse supernova neutrinos; sensitivity to neutrinos from a supernova burst, with directional sensi-

tivity; sensitive searches for nucleon decay in modes complementary to LAr; and, ultimately, a search for neutrinoless double beta decay (NLDBD), with sensitivity reaching the normal ordering regime of neutrino mass phase space.

Table 3 summarizes the physics reach of THEIA. The full description of the analysis in each case can be found in [**?**].

Table 3: THEIA physics reach. Exposure is listed in terms of the fiducial volume assumed for each analysis. For NLDBD the target mass assumed is the mass of the candidate isotope within the fiducial volume (assumed to be housed within an inner containment vessel).

Primary Physics Goal	**Reach**	**Exposure (Assumptions)**
Long-baseline oscillations	Equivalent to 10-kt LAr module (Fig. 19)	127 kt-MW-yr
Supernova burst	$< 2^\circ$ pointing accuracy 5,000 events	25-kt detector, 10 kpc
DSNB	5σ discovery	125 kt-yr (5 yrs)
CNO neutrino flux	$< 10\%$	62.5 kt-yr (5 yrs, 50% fid. vol.)
Reactor neutrino detection	2000 events	100 kt-yr (5 yrs, 80% fid. vol.)
Geo neutrino detection	2650 events	100 kt-yr (5 yrs, 80% fid. vol.)
NLDBD	$T_{1/2} > 1.1 \times 10^{28}$ yr	211 ton-yr ^{130}Te
Nucleon decay $p \to \overline{\nu} K^+$	$T > 1.11 \times 10^{34}$ yr (90% CL)	170 kt-yr (10 yrs, 17-kt fid. vol.)
Nucleon decay $p \to 3\nu$	$T > 1.21 \times 10^{32}$ yr (90% CL)	170 kt-yr (10 yrs, 17-kt fid. vol.)

3.5.2 CPV sensitivity

Deployment of THEIA at LBNF would offer excellent sensitivity to neutrino oscillation parameters, including CP violation. Advances in Cherenkov ring imaging techniques lead to improved particle identification and ring counting, which greatly improves background rejection. The fiTQun event reconstruction package, fully implemented in the most recent T2K analyses [**?**], was used for THEIA sensitivity studies. Improvements include a Boosted Decision Tree. Full details can be found in [**?**]. Sensitivity to neutrino oscillation is enhanced by:

1. Improved particle identification using boosted decision trees removes 75% of the neutral current background, relative to the previous analysis, due to improvements in the detection of the faint second ring in boosted π^0 decays;

2. Improved electron/muon particle identification allows for an additional sample of 1-ring, one-Michel-electron events from ν_e-CCπ^+ interactions, without significant contamination from ν_μ backgrounds

3. Multi-ring ν_e event samples can now be selected with sufficient purity to further enhance sensitivity to neutrino oscillation parameters.

The sensitivity to long-baseline physics at THEIA is seen to be comparable to the sensitivity of an equivalently-sized DUNE module [**?**, **?**, **?**], as shown in Fig. 19. This analysis assumes a sufficiently capable near detector (Sec. 4.4). This analysis does not yet make use of the additional information potentially offered by the scintillation component, which can provide tagging of neutrons and other sub-Cherenkov threshold particles, for improved event identification and enhanced calorimetry.

The ability to measure long-baseline neutrino oscillations with a distinct set of detector systematic uncertainties and neutrino interaction uncertainties relative to the liquid argon detectors would provide an important independent cross-check of the extracted oscillation parameter values. In addition, it could provide important insights in comparisons with HK results. DUNE and HK have different baselines, different beam spectra, and different target media. The THEIA target is similar to that used in HK, and could therefore provide additional information to understand the inevitable comparisons.

3.5.3 Hybrid detection concept

THEIA is a proposed hybrid optical detector, capable of separating scintillation and Cherenkov light via use of Water-based Liquid Scintillator (WbLS), fast timing, and spectral sorting. Operating deep underground, THEIA would open up new areas of science, as detailed in the White Paper [**?**] and summarized below.

Cherenkov light offers electron / muon discrimination at high energy via ring imaging, and sensitivity to particle direction at low energy. The scintillation signature offers improved energy and vertex resolution, particle identification (PID) capability via species-dependent quenching effects on the time profile, and low-threshold (sub-Cherenkov-threshold) particle detection. The combination boasts an additional handle on PID from the relative intensity of the two signals.

This detector would offer excellent energy resolution for high-energy neutrino interactions (better than 10% neutrino energy resolution achieved with preliminary algorithms), along with access to a rich program of low-energy, rare-event, and precision physics.

This is likely a cost-effective option, particularly of those designed to broaden the physics program, thanks to the relatively simple and well-understood detector design, without the need for a cryostat or field cage.

A conceptual view of the detector is shown in Fig. 19.

3.5.4 Technology Readiness Level

The THEIA reference design makes use of a number of novel technologies to achieve successful hybrid event detection. Water-based liquid scintillator (WbLS) [**?**] is used to enhance the Cherenkov signal by reducing and potentially delaying the scintillation component. The use of angular, timing, and spectral information offers discrimination between Cherenkov and scintillation light for both low- and high-energy events. Fast photon detectors – such as the 8" PMTs now manufactured by Hamamatsu, which have better than 500-ps transit time spread – will be coupled with spectral sorting achieved via use of dichroic filters [**?**].

Successful separation of Cherenkov and scintillation has been demonstrated even in a standard scintillator like LAB-PPO [**?**] with the use of sufficiently fast photon detectors, and will

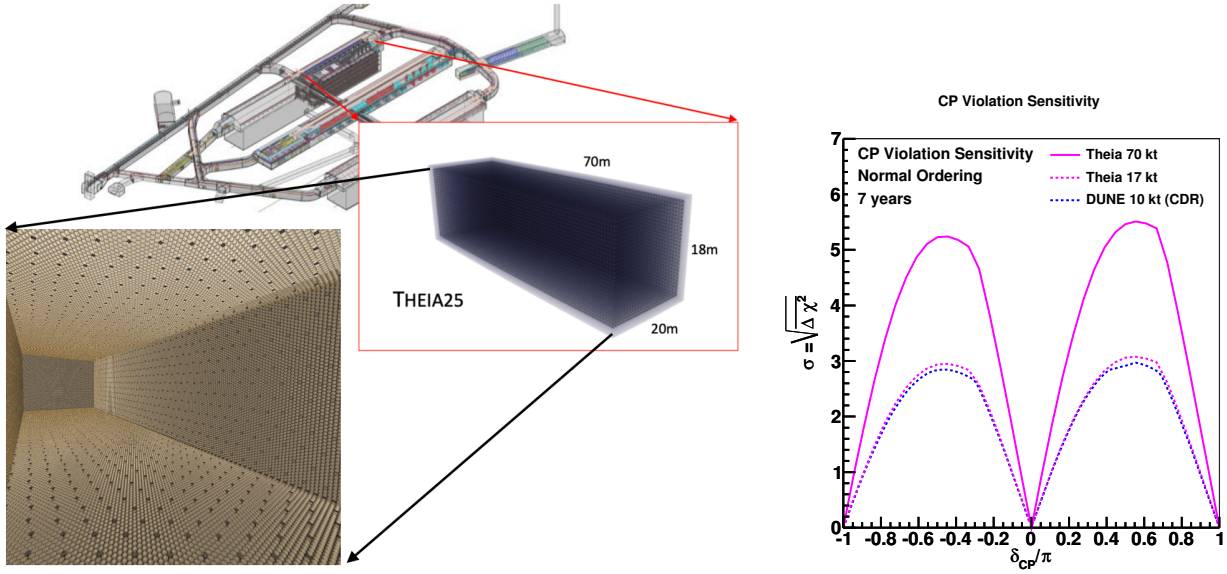

Figure 19: *Left panel:* THEIA-25 sited in the planned fourth DUNE cavern, with an interior view of THEIA-25 modeled using the Chroma optical simulation package [?]. Taken from [?]. *Right panel:* Sensitivity to CP violation (i.e.: determination that $\delta_{CP} \neq 0$ or π) as a function of the true value of δ_{CP}, for the THEIA 70-kt fiducial volume detector (pink). Also shown are sensitivity curves for a 10-kt (fiducial) LArTPC (blue dashed) compared to a 17-kt (fiducial) THEIA-25 WCD detector (pink dashed). Seven years of exposure to the LBNF beam with equal running in neutrino and antineutrino mode is assumed. LArTPC sensitivity is based on detector performance described by [?].

be even more powerful when coupled with the WbLS and spectral sorting capabilities planned for THEIA.

Radio-purity in excess of the requirements for the THEIA low-energy program have been demonstrated by successfully operated water Cherenkov experiments (SNO) and scintillator experiments (Borexino).

Further optimization of the design could be achieved by considering deployment of LAPPDs (Large Area Picosecond Photo-Detectors) [?, ?], for improved vertex resolution, or slow scintillators [?, ?] to provide further separation of the prompt Cherenkov component from the slower scintillation. A more complete discussion of the relevant technology, including a number of prototype experiments planned or under construction, is provided in the NF10 Snowmass white paper on "Future Advances in Photon-Based Neutrino Detectors" [?].

The R&D for THEIA will be completed with the successful operation of a number of technology demonstrators currently under construction: (i) a 1-ton test tank and 30-ton engineering and optics study at BNL will demonstrate the required properties and handling of the scintillator; (ii) a low-energy performance demonstrator, EOS, at LBNL [?] will demonstrate the performance capabilities of the scintillator, fast photon detectors, and spectral sorting; and (iii) a high-energy demonstration at ANNIE, at FNAL, will demonstrate GeV-scale neutrino

detection using hybrid technology [**?**]. These detectors are all currently operational, or due to be so by summer 2024. Following results from these demonstrators (FY25), optimization of the conceptual THEIA detector design can be completed (FY26), ready for a preliminary design by FY27.

3.6 FD3 and FD4 detector integration (Stefan, Michel, Sowjanya)

Sketch of complete detector solutions for FD3/FD4. Main options.

3.7 R&D Roadmap (Stefan, Michel, Sowjanya)

Critical technical elements to be tested during R&D. Staged prototyping at CERN Neutrino Platform and elsewhere. Based on input Mary has gathered for P5.

4 The DUNE Phase II Near Detector

Patrick to synthesise what is here already into this list:

- Limitations of phase 1 ND intrinsic in it being a small LAr detector
- Problems previous experiments have had
- Ways gas argon concept answers some of the limitations of phase 1
- BSM opportunities given you are making a low density detector (Silvia's HNL plot)
- try something about prism vs gar (sensitivity vs model independence)

In Phase II, DUNE will have accumulated Far Detector statistics of several thousand oscillated ν_es, resulting in few-percent level statistical uncertainties on the number of electron appearance events. The ultimate physics reach of DUNE will be driven by the systematic constraints, and thus by the performance of the Near Detector. This section will outline some fundamental limitations of the Phase I Near Detector, issues previous experiments have had that it will be important for DUNE to be robust against, and how a gaseous argon detector covers the issues that we are aware of. Furthermore, the beyond standard model (BSM) opportunities of a gaseous argon detector situated downstream of one of the most powerful proton beam dump targets in the world.

To understand the needs of the Phase II ND we must first understand he Phase I ND. ND Phase I consists of two measurement systems which contribute to these constraints, ND-LAr and its muon spectrometer TMS, and SAND.

ND-LAr and TMS are designed to measure neutrino-argon interactions with detector response similar to the FD. Like the FD, ND-LAr+TMS measures muons primarily by range (stopping either in ND-LAr or TMS), and measures both electromagnetic showers and hadrons calorimetrically. While ND-LAr is smaller than the FD, the dimensions of ND-LAr are optimized to contain a large fraction of hadronic particles produced in neutrino interactions.

ND-LAr+TMS is able to reconstruct the same observables as the FD, with essentially the same resolution. The magnetization of TMS further allows constraints on the wrong-sign events, which is especially important in antineutrino mode, although this constraint is only available in the energy and angular range where the lepton reaches TMS. ND-LAr+TMS move off axis to collect data in different fluxes, and directly constrain the energy dependence of neutrino cross sections. SAND is permanently on-axis, and measures neutrino cross sections on various nuclear targets while also monitoring the beam. SAND has a LAr target, so that it can also measure cross section ratios including argon.

To ensure that DUNE is not systematically limited, it is important to plan for a potential ND upgrade as part of Phase II. The upgrade should address the limitations of the Phase I ND. This is a difficult challenge as the ultimate performance of the Phase I ND is not yet understood, and will depend on analysis techniques developed over the coming decades. However, potential fundamental limitations of the Phase I ND include

- Identification of exclusive final states,
- Identification of low-energy hadrons, especially protons,
- Modeling the acceptance correction for hadronic containment and high angle events not covered by TMS,
- Neutral particle identification and measurement
- Sign-selection of low-energy muons and hadrons of all energies.

ND-LAr is an excellent detector for identifying exclusive final states when all hadrons are above threshold, those hadrons do not undergo strong interactions in the detector and the lepton is fully reconstructed. However, many events in the DUNE energy range have pions with hundreds of MeV of kinetic energy, which travel several interaction lengths and frequently undergo interactions depositing energy in the nuclei of atoms that is then not seen in a calorimetric energy reconstruction. Furthermore, below threshold pions decay to final states including neutrinos leading to large fractions of their rest mass not being visible calorimetrically. Looking also at protons, observing very low-energy protons is an excellent way for our analysis to be sensitive to nuclear effects, and this is challenging due to the density of LAr and the threshold. ND-LAr will also have many events that are poorly contained and thus the hadronic energy is poorly measured. These are fundamental limitations of small liquid argon TPCs, not addressable with improved reconstruction techniques. The movable detector concept can ameliorate some of these issues, but issues like acceptance corrections are a remaining fundamental difference between the ND and FD. Due to all of these effects, it will be necessary to make model-dependent corrections to the hadronic energy which will have potentially significant systematic uncertainties.

A further issue is that sign selection is possible only for muons that enter the magnetized TMS, which places a threshold of approximately 800 MeV, below which muons will not be charged analyzed. The sign of electrons and charged pions will not generally be measured at all. Some of these limitations can be addressed by SAND, which is magnetized. For particles in

the low-density CH_2 tracker, SAND has low thresholds and excellent PID, with sign selection via curvature and very low rates of hadron interactions. However, extrapolations between target nuclei are not well controlled in modern neutrino interaction uncertainty parameterisations, and differ significantly from model to model so using data taken on non-argon targets introduces model dependence and significant systematic uncertainties. It is therefore not clear how useful measurements on hydrocarbon are for predicting argon interactions, and the LAr target of SAND is planned to be instrumented optically, and it is not demonstrated that low-threshold PID is possible.

Examples of where similar issues have been impactful in previous long-baseline experiments can be seen from the T2K experiment. T2K uses a near detector system with a a magnetised tracker upstream and downstream of two primarily hydrocarbon targets. The system has fairly high hadron reconstruction thresholds and poor acceptance for particles at high angles to the beam direction (See Figure 20). T2K's far detector by contrast is a water Cherenkov detector with even higher hadron reconstruction thresholds but 4π acceptance. In order to remedy this, T2K has found it necessary to upgrade its near detector to reduce hadron energy thresholds and increase high-angle acceptance [40]. T2K also provides an example of the need for a near detector that can study interaction models in detail. While within-model interaction systematics contribute a large fraction of T2K's systematic uncertainty budget, more significant are model-to-model differences. In these cases even if the nominal model used in the analysis has small systematic uncertainties, there may be alternate models that cannot be ruled out that necessitate large hard to parameterise uncertainties being added. Being able to compare these models in kinematic regions where they differ most such as the low-momentum proton regime described above enables entire models to be ruled out and the systematic uncertainty in the region of interest reduced. A final example of the ability to precisely constrain neutrino interactions is the case where your analysis sees that the simulation is unable to describe the data well. While its significance has since reduced, T2K saw an excess in a data sample targeting events with pion activity. 14 events were seen when only $\sim$7 were expected. Without detector components able to study pion production models in detail on the same target nucleus in the same energy range it was not possible to determine whether this excess was problematic or not.

To address the limitations of the Phase I ND and improve robustness to the issues described above, planning for the Phase II Near Detector is actively underway focused towards a detector which has:

- Argon as the primary target nucleus,
- Very high PID efficiency across a broad kinematic and angular range,
- Low thresholds for protons and pions,
- Magnetization, and 4π acceptance

This will:

- Not introduce any problems with extrapolating between target nuclei

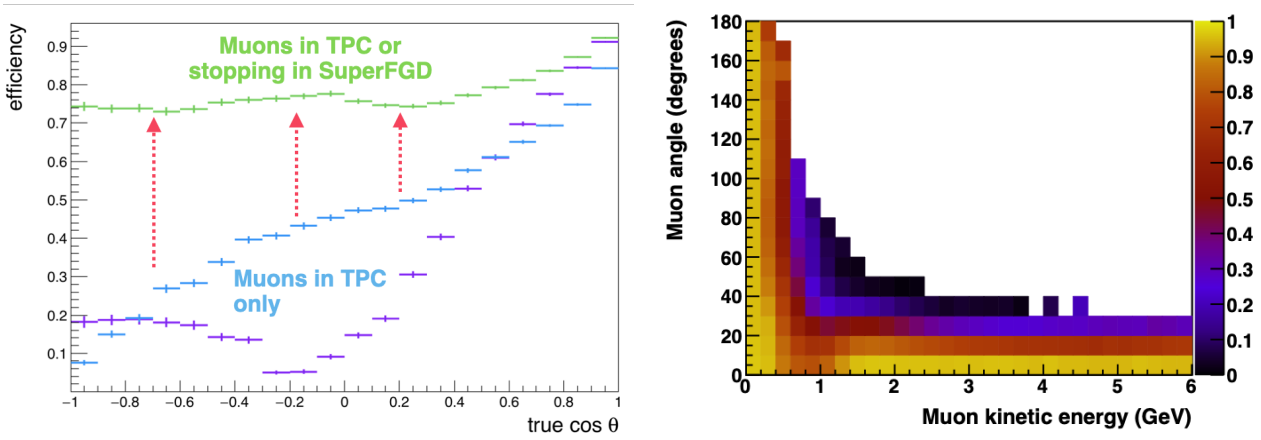

Figure 20: Caption: Left: T2K near detector acceptance before and after upgrade [41]. The purple line shows the initial T2K ND's acceptance, the blue line shows the acceptance after adding one of the upgrade detectors and the green the performance after the full upgrade. Right: Current DUNE Phase I ND acceptance [3].

- Ensure DUNE has no regions where the FD has good acceptance where the ND does not
- Reduce systematics on calorimetric energy reconstruction that are essential when the below threshold hadron spectra are not well measured
- Better constrain wrong-sign backgrounds in the low-energy and high-angle regions
- Enable different models of neutrino interactions to be distinguished in-situ using data from the phase space regions most sensitive to their differences thereby further reducing systematic uncertainties
- Maximise the robustness of DUNE to unexpected differences between data and interaction and flux models including those that cannot be corrected for with the PRISM method

Version written by Chris:

In Phase II, DUNE will have accumulated Far Detector statistics of several thousand oscillated ν_es, resulting in few-percent level statistical uncertainties on the number of electron appearance events. To reach the physics goals of DUNE, a similar level of systematic uncertainty must be achieved, which requires precise constraints from the Near Detector. To understand the needs of the Phase II ND, we must first understand the expected performance of the Phase I ND, which consists of two measurement systems, ND-LAr+TMS, and SAND. This section will describe why the Phase I ND is critical for DUNE physics, and discuss limitations inherent in the design. To ensure that DUNE is not systematically limited, it is important to plan for a potential ND upgrade as part of Phase II. The upgrade should address the limitations of the Phase I ND. This is a difficult challenge as the ultimate performance of the Phase I ND is not yet understood, and will depend on analysis techniques developed over the coming decades.

ND-LAr+TMS is designed to measure neutrino interactions on the same nuclear target as the FD, and with detector response similar to the FD. Neutrino energy in the FD is estimated by summing the lepton energy with the hadronic energy. The FD measures the muon energy by range, and the energies of all other particles calorimetrically. ND-LAr+TMS also measures muons by range, and other particles calorimetrically. ND-LAr+TMS is able to reconstruct the same observables as the FD, and measure them with the essentially the same resolutions, in an unoscillated beam. This capability is the core requirement of the DUNE ND, and will be a critically important constraint for all DUNE long-baseline measurements. ND-LAr+TMS move off axis to collect data in different fluxes, and directly constrain the energy dependence of neutrino cross sections. SAND is permanently on-axis, and measures neutrino cross sections on various nuclear targets while also monitoring the beam. SAND has a LAr target, so that it can also measure cross section ratios including argon.

The dimensions of ND-LAr are not driven by event rate, but rather by containment of electrons and hadrons, so that they can be measured calorimetrically in the same way as the FD. To minimize cost, the dimensions are chosen to be as small as possible while maintaining full coverage of the neutrino-argon phase space. However, this means that the acceptance is non-uniform, and depends on the event kinematics. At higher neutrino energies, most events are poorly contained in ND-LAr.

TMS is able to provide sign selection of muons, which is especially important to reject wrong-sign background in antineutrino mode. However, ND-LAr itself is not magnetized, so the sign selection is only possible for muons which enter TMS, and there is no sign selection for other particles. SAND will be able to measure the sign of all charged particles in its low-density CH_2 tracker, but not generally for hadrons produced in the argon target.

To constrain neutrino-argon modeling, it is useful to identify specific exclusive processes, especially because about two thirds of neutrino interactions in DUNE will have pions in the final state. ND-LAr is an excellent detector for identifying pions and protons when they are above threshold, and do not undergo strong interactions inside the detector. However, many events in the DUNE energy range have pions with hundreds of MeV kinetic energy, which travel several interaction lengths and frequently scatter. Also, protons below about 400 MeV/c are impossible to detect because they travel only a few mm, and highly saturated ionization charge is recorded on a single pixel.

These limitations motivate the design of the Phase II ND. Specifically, the Phase II ND should have

- argon as the primary target nucleus,
- very high particle ID efficiency across a broad range of energy and angle,
- low thresholds for protons and pions,
- magnetization, to achieve 4π acceptance and sign selection.

Employing an argon target will ensure that constraints from the Phase II ND can be applied directly to the argon FD without any extrapolation in atomic number. A broad acceptance and

high PID will enable exclusive final states to be identified, which will improve the constraints on neutrino interaction modeling. Low thresholds will make the Phase II ND highly sensitive to nuclear effects. Magnetization will ensure sign selection at all energies and angles, for both charged leptons and charged pions.

4.1 Phase II Improved Tracker Concept

A gaseous argon-based time projection chamber (gaseous-argon TPC, or GArTPC) can reconstruct pions and protons with lower detection thresholds than a liquid-argon TPC. This can be seen in Figure 21, which compares the same simulated event in a liquid argon TPC and a gaseous argon TPC. The protons travel a much longer distance and can be more clearly separated in gaseous argon. The GArTPC is also less susceptible to confusion of primary and secondary interactions, since secondary interactions occur infrequently in the lower density gas detector. If the TPC is inside a magnet, it can better distinguish neutrinos and anti-neutrinos and can determine the momenta of particles that range out of the detector. It can also measure neutrino interactions over all directions, unlike the ND-LAr, which loses acceptance at high angles with respect to the beam direction. Therefore, a gaseous-argon TPC provides a valuable and complementary sample of argon interactions to better understand neutrino-argon interactions.

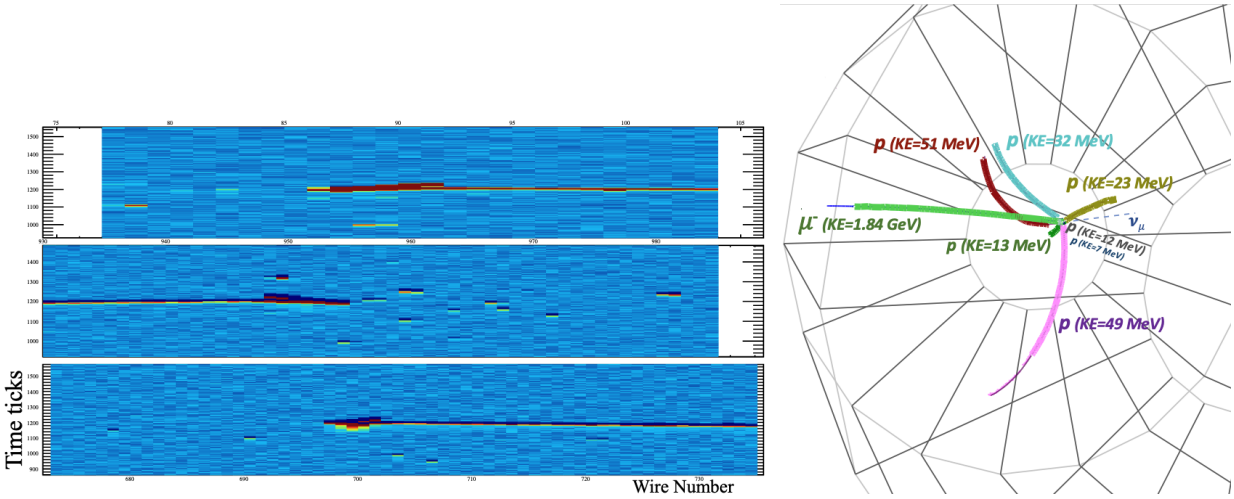

Figure 21: The two images above show the same simulated multi-proton event in a liquid argon TPC (on the left) and a gaseous argon TPC (on the right).

However, a downside to a gaseous argon TPC is the lower neutrino event rate in a given volume due to the lower density. One way to improve this is to use high-pressure argon gas. A cylindrical volume with a diameter of roughly 5 m and a length of roughly 5 m and gas at 10 bar would have a fiducial mass of nearly 1 ton of argon, yielding approximately 1 million neutrino interactions per year.

This detector concept is motivated by the considerations in Section 4. Given that a detector of this type is desirable to satisfy the requirements listed above there are also significant oppor-

tunities to study BSM physics. Particularly, many BSM processes involve long-lived particles created when DUNE's proton beam is impinged on the beam dump. These long-lived particles then subsequently decay with a rate proportional to the volume of the detector used to study them. By contrast the standard model backgrounds to these processes are due to interactions and so are proportional to the mass of the detector. A high-volume low-mass gas detector is therefore ideally suited to study these signatures. Two of the most promising are heavy neutral leptons (HNLs) and anomalous tau appearance. Particularly in the case of HNLs a gas argon detector at DUNE would have world-leading sensitivity in the lower mass region and for the first time potentially be able to probe the Type I see-saw model region, see Figure 3.

As illustrated in Figure 22, the baseline concept for the ND-GAr detector comprises:

1. A pressurised gaseous argon TPC
2. A surrounding calorimeter
3. A magnet
4. A muon-tagging system

A light-collection system may prove necessary to reduce pileup and provide to t_0 for the drift time for events that do not reach the calorimeter. The entire ND-GAr system will move transverse to the beam with ND-LAr as part of the DUNE-PRISM concept.

4.1.1 TPC Charge Readout

There are a variety of techniques that can be used to amplify and collect the drifting electrons, and the options currently under consideration for ND-GAr will be briefly presented here. However, the gas gain decreases as the gas pressure increases. High pressure argon gas mixtures have been used in past, such as in the PEP-4 detector at SLAC [42] which used a (flammable) gas mixture of 80:20 Ar-CH_4, operated at 8.5 atm. For the DUNE ND-GAr R&D to ensure adequate stability and gain in a non-flammable gas with a high argon fraction.

Multi-Wire Proportional Chambers Tanaz

In order to collect sufficient event statistics, DUNE's gas-argon-based TPC, HPgTPC, at the core of ND-GAr, must be both large and capable of functioning under high pressures. A TPC of the size used in the ALICE experiment at CERN may be adequate in terms of size, but only if the gas inside is pressurized to approximately 10 atmospheres. As it so happens, as a result of the recent upgrade of ALICE's readout system to GEMs, the previously operated ALICE multi-wire proportional chambers, MWPCs, have become available. These MWPCs previously operated within ALICE at 1atmosphere, hence their operation needed to be assessed within a high-pressure argon gas environment.

Two test stands in the UK and the USA have been tasked with testing the ALICE chambers under high pressure, the Gas-argon Operation of ALICE TPC, GOAT, and the Test of Overpressure Argon Detector, TOAD. GOAT utilized a pressure vessel rated to 10 atmospheres and tested an ALICE inner chamber for its achievable gas gain at various pressure setpoints,

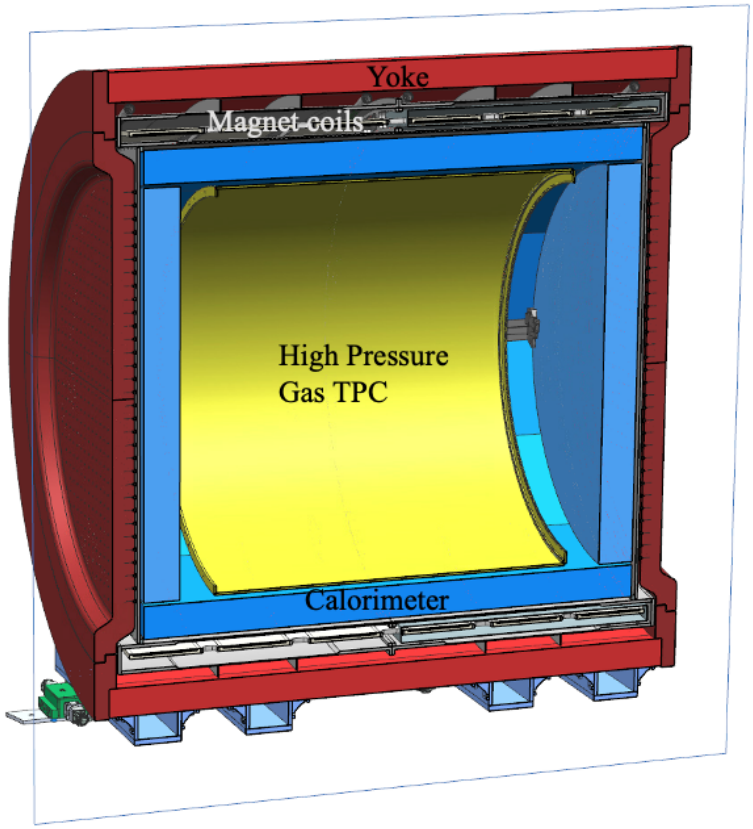

Figure 22: Cutaway view of the full ND-GAr detector system showing the HPgTPC, the calorimeter, the magnet, and the iron yoke. The detectors for the muon-tagging system are not shown.

amplification voltages, and gas mixtures. TOAD previously tested an ALICE outer chamber for its achievable gas gain up to 5 atmospheres, and currently, it is being commissioned in Fermilab Test Beam Facility, FTBF for its test beam data taking and for performing a full slice test of the electronics and DAQ. In both test stands, wire-based readout chambers have been tested in high-pressure environments, demonstrating that they can provide reasonable gas gains when they operate at or above the high voltage values previously operated at in ALICE. Despite this, the long-term operation and stability of these chambers at such high voltages remain to be investigated. There are also plans to test MPGD-based charge readout systems such as GEMs, as described in the paragraph that follows.

TPC Readout with THGEMS -Kostas

In a TPC using GEMS/THGEMs the ionization drift electrons enter the THGEM holes and are accelerated within a high electric field. At sufficiently high fields, this acceleration causes the electrons to further ionise the gas medium, resulting in a Townsend discharge. This exponentially increases the number of electrons and therefor the signal. Typically, THGEMs

are produce from epoxy laminate/FR4 substrates which have some limitations. We propose to use a new type of THGEMs made out of glass. These glass THGEMs developed at Liverpool are fabricated using a new manufacturing method whereby, a masked abrasive machining process is used [28]. The innovation allows for customisation of glass THGEMs, where both substrate and electrode materials can be tailored depending on our requirements including high stiffness, low outgassing and resilience to damage from discharges. The amplified electrons from the THGEMs would be readout on a segmented anode to allow for tracking reconstruction.

TPC Readout electronics Patrick or Ioannis?

Due to the high-pressure nature of this detector we must develop readout electronics that can operate inside the pressure vessel so as to minimise the analogue signal path. These electronics must also be zero-supporessed and compatible with the existing DUNE DAQ infrastructure for the Phase I ND. Readout electronics has traditionally been one of the cost drivers of TPCs. While the pixel size of the final detector has not been determined, detectors like ALICE had 700k channels. With this number of channels work is needed for this detector to ensure that the electronics system is cost- effective. R&D work is underway in the UK and USA to deliver such electronics, with early work delivering a prototype system using the SAMPA ASIC plus FPGA-based control and aggregation already in hand that would cost £2M if scaled up to the full detector.

4.1.2 Calorimeter

- Alfons The gaseous TPC will be excellent measuring the track of charge particles, but to first order is blind to neutral particles. As such it is important to have a system that can detect these. At neutrino energies of a a few GeV these are mostly photons (for example from π^0-decays) and neutrons existing the nucleus in the energy range from below 100 MeV to GeV. The energy of photons will be determined calorimetrically, while the neutron energy can be determined by measuring its time of flight between the production vertex and a nuclear re-scatter in the calorimeter (see [43] for more details). Both particles will be key to measuring nuclear effects that will influence the relationship between true and reconstructed energy and the dynamics of the neutrino interactions. It is also the case that the HPgTPC should occupy the largest possible volume and the calorimeter has to surround the TPC. As such it has a rather large surface area even for modern particle physics detectors. Optimising this detector to achieve the physics goals whilst still being affordable is a key task of the gaseous argon detector group.

A possible affordable technology with the required performance is based on a plastic scintillator sampling calorimeter that is constructed from active tile layers using a combination of the technology developed by the CALICE R&D Collaboration [44] and the more traditional scintillator strip, WLS-fibre and SiPM readout used in traditional neutrino experiments, like the T2K near detector. The general structure of the calorimeter can be seen in Figure 22 and Figure 23(left).

The default barrel geometry consists of 60 layers with the following layout:

- 8 layers of 2 mm copper + 5 mm of 2.5 $\times$ 2.5 cm^2 tiles + 1 mm FR4

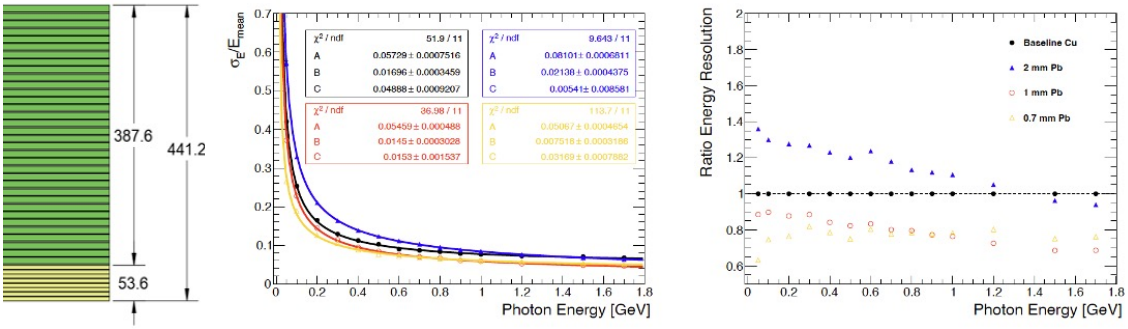

Figure 23: Left: Possible structure of a combined tile and strip layer sampling calorimeter. Towards the TPC there are several tile/absorber layers (yellow), which are followed by strip/absorber layers (green). Middle: energy resolution as a function of photon energy for different absorber configurations. The function $\frac{\sigma_E}{E} = \frac{A}{\oplus}\sqrt{E} \oplus \frac{B}{E}C$ has been fitted to the simulated data. Right: Ratio of the energy resolution for the differnt absorber configurations. The best resolution is achieved using thin lead absorber. The overall depth of the ECAL has been kept constant. More details can be found in [3].

- 52 layers of 2 mm copper + 5 mm of cross-strips 4 cm wide

For the present study, copper has been chosen as the absorber material as initial studies have shown that this material provides a good compromise between calorimeter compactness, energy and angular resolution. It also allows for the removal of heat generated by the electronics in the tile layer.

More details of the detector layout and an initial performance evaluation for photons are summarised in Figure 23. There are several possible readout ASICs on the market to determine the time and charge of the SiPM signals, one possibility would be the KLauS ASIC [45].

4.1.3 Muon System

A gaseous argon near detector will need a system outside the calorimeter to improve pion/muon separation. The muon tagger would likely be composed of well-established current technologies, such as a coarsely instrumented scintillator detector. It is not likely to require substantial R&D, but will need engineering effort.

4.1.4 Magnet Concept

In order to fulfill the physics goals, the TPC volume of the Near Detector must be magnetized to measure muons and other particles momenta and determine the sign of their charge. The magnetized system will analyze both the tracks originating from ND-LAr and penetrating from upstream and the tracks produced within the magnetic volume by neutrino interactions.

The need to make the magnet as compact as possible and minimize the material at the end of the TPC and in front of the calorimeter suggest an integrated design in which the magnet structure serves also as a pressure vessel for the TPC gas volume. The magnetic design described in [**?**] and summerized here fulfils these requirements.

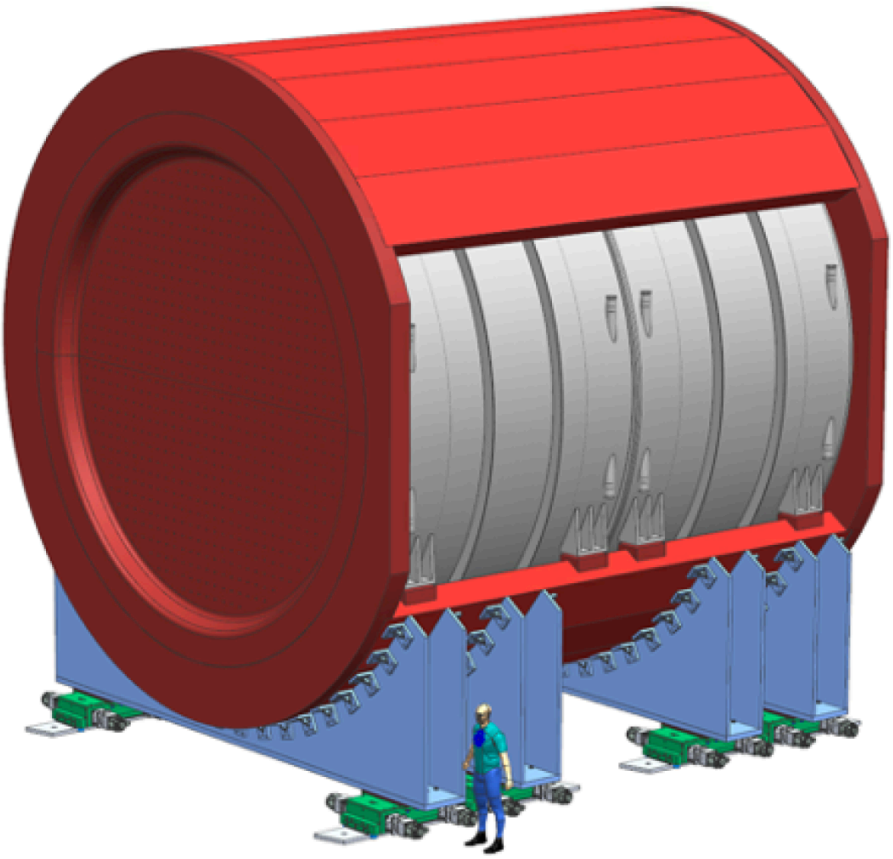

Figure 24: The SPY magnet system. The cut is upstream, to minimize material traversed by tracks originating from neutrino interactions in Nd-LAr.

The magnet system consists of a superconducting solenoid surrounded by an iron return yoke. To limit the size and cost of the system, the design integrates the superconducting solenoid cryostat so that it will also serve as a pressure vessel body for the High Pressure TPC (HPgTPC) and the support for the HPgTPC and calorimeter elements located in its bore.

Additionally, the design of the iron magnet yoke uses the mechanical strength of the yoke's pole faces to eliminate the large domed heads that would normally be required for a large-diameter pressure vessel.

An important design requirement for ND-GAr is the ability to accurately measure the momentum of muons that originated in ND-LAr. This requirement limits the amount of material allowed on the upstream side of ND-GAr and forces us to adopt a non conventional and unsymmetrical iron yoke. An iron yoke that eliminates a portion of the iron along the entering particle paths was developed and designed. The system is called SPY – Solenoid with Partial return Yoke.

A schematic of ND-GAr is shown in Figure **??** where the missing section of the yoke is shown. A cut-away view is shown in Figure **??** which shows the coils, ECAL components,and

the HPgTPC.

The complete design of SPY is given in [**?**]. We summarize here the main requirements and the main technological features:

- The momentum analyzing power of ND-GAr assembly (magnet + TPC) must provide at least 3% momentum resolution for the muons originating within ND-LAr. Besides, for particles produced as a result of neutrino interactions in the argon high pressure gas TPC, the analyzing power must produce a resolution in neutrino energy reconstruction at least as good as that of the DUNE far detector.

- The magnetic field uniformity, thanks to recent and relevant improvements in the capability of software reconstructions, is not required to be very high. $\pm 10\%$ variation within the magnetic volume is expected to be sufficient, provided that a very accurate map is measured on the magnet "as built". However, it's worth emphasizing that the magnet design fully described in [**?**] largely exceeds the $\pm 10\%$ requirement, offering $\pm 1\%$ variation over the whole volume. Careful studies were also done to evaluate and minimize the magnetic forces between Nd-Gar and SAND.

- The superconductor will be co-extruded in high purity aluminum to provide quench protection in the worst case. A possible solution for the cable, based on Niobium Titanium, is the current baseline but higher temperature superconductors such as MgB_2 will also be considered in the future. An R&D program is in progress in this direction.

- ND-GAr must provide good acceptance for muons exiting ND-LAr and must fit within the space constraints imposed by the Near Detector hall design and by the need to be movable in agreement with the PRISMA concept.

- ND-GAr's magnet system must present as little material as possible in the path of the muons exiting from ND-LAr and must have a minimum quantity of material in the downstream face of the yoke to assist in the discrimination of muons from pions.

- The vacuum cryostat must be capable of providing mechanical support and cryogenic environment for the superconducting coils. Besides, the inner wall of the vacuum cryostat must be sufficiently strong to serve as the outer wall of the pressure vessel for the HPgTPC and support the weight of ECAL.

- The carbon steel of the return yoke must be designed to provide a uniform 0.5 magnetic field over the whole length of the solenoid and limit fringe fields to the levels required by the experiment and by the co-existence with SAND. Last but not least, provide flat carbon steel pole tips for the magnet return yoke that match the magnetic field boundary conditions at the ends of the solenoid and provide the mechanical support for the pressure vessel end flanges.

Taking into account all the requirements outlined and summarised above, the preliminary but complete design of SPY described in [**?**] was completed. We simply summarize the main parameters achieved in the current design, which all meet or exceed requirements, in Table below.

Parameter	Value	Notes
Central field	0.5 T	
Field uniformity	±10%	Current design achieves ±2%
Ramp time to full field	30 min	
Stray field	≤0.01 T	
Bore	6.725 m	Stray field in SAND negligible, in LAr FV ≃ 10 G
Diameter	7.85 m	Reduction possible with TPC and ECAL optimizations
Length	≃ 7.8 m	Cryostat diameter at stiffening rings
Solenoid weight	≃ 150 t	
Yoke total weight	≃ 757 t	

Table 4: List of SPY parameters according to current preliminary design.

4.1.5 Light Detection Options

- Add mention of tracking
- Add mention that needs to move to GEMs from wires

Enabling time-tagging by the TPC would provide an absolute determination of the vertex position and interaction time, thus simplifying the matching with external detectors and enabling reconstruction of interactions whose byproducts range-out before reaching them. The only demonstrated technique to accomplish this in TPCs is through the use of primary scintillation. The complexity of the system used for this requires significant R&D, primarily studying the level of localisation needed in order to associate time information with a given interaction. The choice of gas mixture for the detector will also be key as different mixes have very different scintillation properties [46, 47].

Although pure argon gas emits scintillation light copiously at the level of 20000 ph/MeV, gases employed historically in TPCs when used for accurate tracking in magnetic fields do not [48]. The recent demonstration of strong (and fast) wavelength-shifting in the Ar/CF_4 system, with yields in the range 700-1400 ph/MeV [49], opens the possibility of ns-level time tagging for energy deposits down to 5 MeV, at least [50, 51].

In view of the requirements for single-photon detection, magnetic field compatibility and, given the spectral range of the scintillation, two technologies are of particular interest as described below. Light readout of secondary scintillation at the amplification stage is also an option that should be explored.

SiPMs SiPMs are well suited for detection in the visible range, and several ganging schemes are available nowadays for large area coverage (e.g., [52]). Silicon suffers from high dark rate at room temperature and, in fact, simulations performed in [50] point to the need of cryogenic operation (-25 deg) to reach MeV-thresholds in ND-GAr. Methods to do this must be studied.

LAPPDs Large-Area Picosecond Photo-Detectors (LAPPDs) are novel photosensors based on microchannel plate technology. With sensitive regions of order 20 by 20 cm and sub-cm position resolution, these detectors are a good candidate for covering large areas. They are tolerant of magnetic fields and handle sub-nanosecond timing with excellent signal to noise ratio, without any cooling requirements. LAPPDs were recently demonstrated to work for neutrino detection by the ANNIE experiment. Ideal coverage could be achieved with order of 100 LAPPDs which could be delivered within a few years at current production rates. Depending on the choice of quencher/wavelength shifter, modifying the photocathode composition or a wavelength shifter coating might be required.

Studies to optimize this system are required, and include determining optimal coverage, the best photocathode design, and enclosures to allow the LAPPDs to operate at high pressure.

4.1.6 Other ND considerations

If a non-argon-based technology is chosen for Module 3 and/or 4 in Phase II, then it might also prove necessary to incorporate some of that material into ND-GAr. One possibility is to replace some or all of the upstream calorimeter with similar material to the chosen technology.

4.2 Phase II Improvements to ND-LAr

[Saba or Michele or Dan?]
ND-LAr is the Liquid Argon component of the DUNE near detector complex. With the intense neutrino flux and high event rate at the ND, traditional, monolithic, projective wire readout liquid argon time-projection chambers (LArTPCs) would be stretched beyond their performance limits. To overcome this hurdle, in ND-LAr, it is proposed to fabricate a large TPC out of a matrix of smaller, optically isolated TPCs read out individually via a pixelized readout. The subdivision of the volume into many smaller TPCs allows for shorter drift distances and times. This and the optical isolation lead to fewer problems with overlapping interactions.
ND-LAr design consists of 35 optically separated LArTPC modules that allow for independent identification of ν-Ar interactions in an intense beam environment using optical timing. Each TPC consists of a high voltage cathode, a low profile field cage that minimize the amount of inactive material between modules, a light collection system, and a pixel based charge readout. One key aspect of ND-LAr operation is the ability to cope with a large number of neutrino interactions in each spill. The LBNF neutrino beam consists of a 10 us wide spill, with $\mathcal{O}$(ns) bunch structure, delivered at a $\sim$1 Hz rate. This means that there will be $\mathcal{O}(50)$ nu interactions per spill in phase one and $\mathcal{O}(100)$ nu interactions per spill in phase two. Given the relatively low expected cosmic ray rate during the beam (estimated to be $\sim$0.3/spill at 60-m depth), this beam related pile-up is the primary challenge confronting the reconstruction of the ND-LAr events. The 3D pixel charge will be read out continuously. The slow drifting electrons (with charge from the cathode taking $\sim$300 μs to arrive across the 50 cm distance) will be read out with an arrival time accuracy of 200 ns and a corresponding charge amplitude within a $\sim$2 μs wide bin. This coupled with the beam spill width gives a position accuracy of 16 mm. While this is already good spatial positioning, the ND-LAr light system will provide an even more

accurate time-tag of the charge as well as the ability to tag sub-clusters and spatially disassociated charge depositions resulting from neutral particles, such as neutrons, coming from the neutrino interaction. Thus the ND-LAr light system has a different role than that in the FD, as it must time-tag charge signal sub-clusters to enable accurate association of all charge to the proper neutrino event, and to reject pile-up of charge from other neutrino signals.

4.3 Phase II Improvements to SAND

- Alessandro

SAND is a multipurpose detector composed of a Superconductive Solenoid, a high-performance Electromagnetic Calorimeter (ECAL), a light Tracker, and an active Liquid Argon target (GRAIN). The main purpose of the SAND detector will be to monitor the neutrino beam, but it will also be capable of making independent measurements of the neutrino flux and flavor content. This additional capability adds robustness to the Near Detector complex, enabling better control over systematics and background. The Magnet and the ECAL were part of the KLOE detector at INFN-Laboratori Nazionali di Frascati and will be refurbished for Phase I, without the need for upgrades during Phase II. The Tracker, based on Straw Tubes, will be a completely new detector capable of reconstructing charged particle tracks in the magnetic field and studying neutrino cross sections on Carbon and Hydrogen targets. Major upgrades for Phase II are not foreseen.

GRAIN is an innovative LAr detector as it will employ a completely new readout technique, utilizing only scintillation light for track reconstruction. This task is accomplished by cameras with light sensors made of a matrix of Silicon Photomultipliers (SiPMs) and optical elements such as special lenses or Coded Aperture Masks. The GRAIN project is very challenging because, due to the low efficiency of light sensor to VUV scintillation light, the number if photons detected and used by the reconstruction algorithms is low. We will try for the phase II to improve light collection by improving the Photon Detection Efficiency (PDE). For this purpose, we are developing with "Fondazione Bruno Kessler" (FBK-Trento) Backside Illuminated SiPMs (BSI SiPM). In this architecture the light entrance window is on the back of the Silicon while all of metallic contacts are on the front side. This will allow us to improve the fill factor and optimize the anti reflective coating on the entrance window. We plan to substitute all the Matrices of traditional Front Side SiPMs with the new ones, if they will be available and mature for the Phase II.

4.4 Near Detector Options for Non-Argon Far Detectors

In the event that one of the Phase 2 far detectors consists of a neutrino target material that is not argon-based, such as the Theia detector concept described in Section 3.5, the Phase 2 near detector complex will need to provide measurements of neutrino interactions on non-argon target nuclei. Several options exist for modifying the Phase 1 suite of near detectors to make such measurements, including modifying an existing Phase 1 detector (SAND) to incorporate C, O, and H nuclear targets, embedding Water-based Liquid Scintillator (WbLS) targets within

the ECAL of the Phase 2 gaseous argon TPC (GArTPC), and constructing a new, dedicated, water-based near detector.

4.4.1 Installing O/C/H Targets in SAND

The SAND detector is equipped with a modular Straw Tube Tracker (STT) with integrated targets designed to be individually replaceable with different materials. A total of 78 thin planes – each about 1.6% of radiation length X_0 – of various passive materials with high chemical purity and comparable thickness are alternated and dispersed throughout active layers – made of four straw planes – of negligible mass in order to guarantee the same acceptance to final state particles produced in (anti)neutrino interactions. The STT allows to minimize the thickness of individual active layers and to approximate the ideal case of a pure target detector – the targets constitute about 97% of the mass – while keeping the total thickness of the stack comparable to one radiation length and an average density of about 0.17 g/cm^3. The lightness of the tracking straws and the chemical purity of the targets, together with the physical spacing among the individual target planes, make the vertex resolution ($\ll 1$ mm) less critical in associating the interactions to the correct target material. The average momentum resolution expected for muons is $\delta p/p \sim 3.5\%$ and the average angular resolution better than 2 mrad. The momentum scale can be calibrated to about 0.2% using reconstructed $K_0 \to \pi^+\pi^-$ decays. The STT is optimized for the "solid" hydrogen technique, in which $\nu(\bar{\nu})$ interactions on free protons are obtained by subtracting measurements on dedicated graphite (C) targets from those on polypropylene (CH_2) targets. The default target configuration in Phase I includes 70 CH_2 targets and 8 C targets. The use of a distributed target mass within a low-density tracker results in a rather uniform acceptance over the full 4π angle, as shown in Fig. 25. The acceptance difference between different targets can be kept within 10^{-3} for all particles (Fig. 25) thanks to their thinness and their alternation throughout the detector volume. The subtraction procedure between different materials can then be considered model-independent. Furthermore, the detector acceptance effectively cancels out in comparisons among the selected interactions on different target nuclei.

We can obtain concurrently both oxygen and water targets in Phase II by replacing some of the initial CH_2 targets with polyoxymethylene (CH_2O, acetal) planes with the same equivalent thickness in terms of radiation length and nuclear interaction length λ_I. Interactions on oxygen are obtained from a subtraction between CH_2O and CH_2 targets, while interactions on water from a subtraction between CH_2O and C targets. To this end, acetal slabs 4.5mm thick can be used, corresponding to about 0.016 X_0 and 0.008 λ_I. The oxygen content by mass within acetal is dominant at 53.3%. By replacing only 20 polypropylene targets (out of 70) with the equivalent CH_2O ones we can obtain an oxygen target mass of about 760 kg and a water target mass of about 850 kg. Assuming an exposure of 3×10^{21} POT, corresponding to about 2 years with the default beam intensity and to about one year with the upgraded beam, we expect to collect 3×10^6 ν_μ CC events with the FHC beam and 1×10^6 $\bar{\nu}_\mu$ CC events with the RHC beam on oxygen. The subtraction procedure introduces a relatively modest increase around 40% in the statistical uncertainties with respect to the case of ideal targets. The resulting statistical uncertainties are comparable with the expected systematics from the momentum

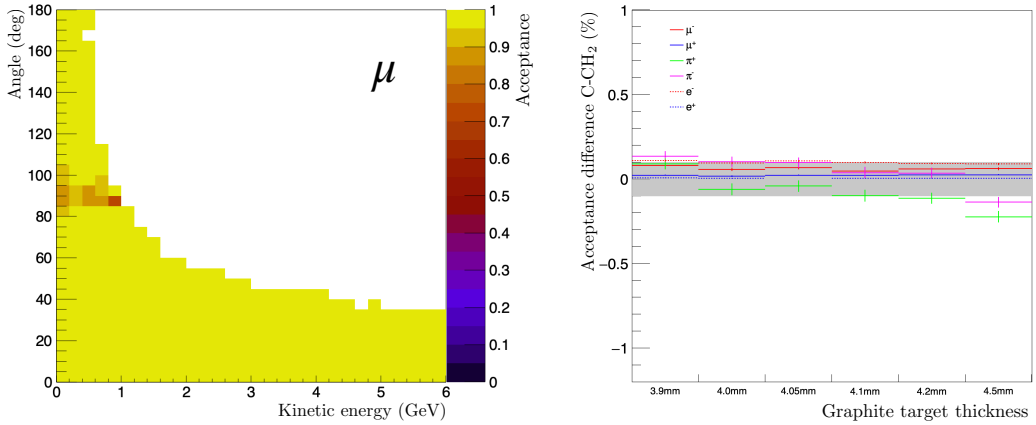

Figure 25: Left plot: Muon acceptance for ν_μ CC interactions in FHC beam in SAND. Right plot: Difference in acceptance between the CH_2 and C targets in SAND.

scale uncertainty of 0.2%.

4.4.2 WbLS Targets in the GArTPC ECAL

The GArTPC described in Section 4.1 is capable of supporting active WbLS targets within the downstream portion of the upstream ECAL, as shown in Figure 26. The WbLS layers would consist of horizontal and vertical bars (similar to the NOνA configuration discussed in the next section), and interactions in the WbLS layers produce particles that enter the high pressure gas TPC where they are precisely tracked. Neutral particles are measured by the surrounding ECAL, and the active WbLS layers provide an additional measure of low energy particles near the interaction vertex ("vertex activity"). For neutrino interactions within the gas TPC, the WbLS layers will form an initial low-density section of the ECAL that can provide fast timing for particles exiting the TPC.

There is sufficient space within the ECAL to include WbLS layers with a thickness of at least 10 cm, which would provide more than a ton of target mass. This would produce O(1M) charged current ν_μ interactions in a 14 week run on-axis, and O(10k) charged current ν_μ interactions in a 2 week run at the furthest off-axis position, both of which would be expected to occur within a nominal DUNE yearly run.

4.4.3 Dedicated Water-based Near Detectors

It is possible to install a detector specifically designed to make measurements for a water-based far detector in the DUNE near detector hall. If a new GArTPC is built, it will serve as the downstream spectrometer for ND-LAr, allowing TMS to be used as a downstream spectrometer for a dedicated Water-based Near Detector (WbND). There is space within the existing near detector hall to add 2 new detectors (GArTPC and WbND), although this would limit the off-axis travel capabilities of the detectors within the hall; this would only be possible if sufficient off-axis data were collected with DUNE Phase 1 such that additional off-axis data are not needed in Phase 2. Another option is to excavate a small, additional section of the cavern just

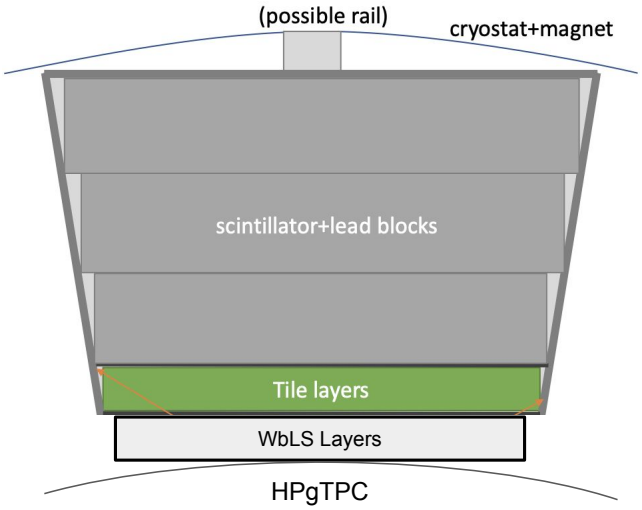

Figure 26: An upstream segment of the GArTPC ECAL is shown (the beam is pointing downward in this picture). The Water-based Liquid Scintillator layers constitute the most downstream portion of the ECAL, and particle produced in these layers via neutrino interactions are tracked in the downstream high-pressure gas TPC.

past the on-axis detector position to produce a new alcove (or "garage") to house the additional detectors (WbND and TMS). The PRISM rail system within the near detector hall would allow these detectors to move on-axis while ND-LAr and GArTPC are in an off-axis position, and to collect off-axis data while the other detectors are on-axis. Finally, it is possible to extend the long dimension of the near detector hall, for a fraction of the cost of the associated far detector, in order to produce additional off-axis travel space that could be used to perform off-axis measurements with WbND.

NOνA-style Near Detector The NOνA near detector consists of individual cells, as shown in Figure 27, arranged in horizontal and vertical layers. The cells consist of PVC extrusions filled with liquid scintillator, and a wavelength shifting fiber collects the light and guides it to the readout avalanche photodiode (APD) [53].

The NOνA near detector design could be used to construct a WbND by replacing the NOνA scintillator with WbLS. The cell size and scintillator fraction of the WbLS would have to be tuned to ensure a high muon reconstruction efficiency. This type of detector would also be capable of a calorimetric measurement of the hadronic energy in the neutrino final state, including better sensitivity to neutrons than a LAr detector, due to the presence of free hydrogen in the target material. This detector technology is well established and would require minimal additional R&D.

LiquidO Near Detector A promising new detector concept for the DUNE ND is based on using opaque scintillators with millimetre-scale scattering length to produce high-resolution images of neutrino interactions. The scintillation photons are stochastically confined close to the point of production via scattering and a lattice of wavelength shifting fibres is

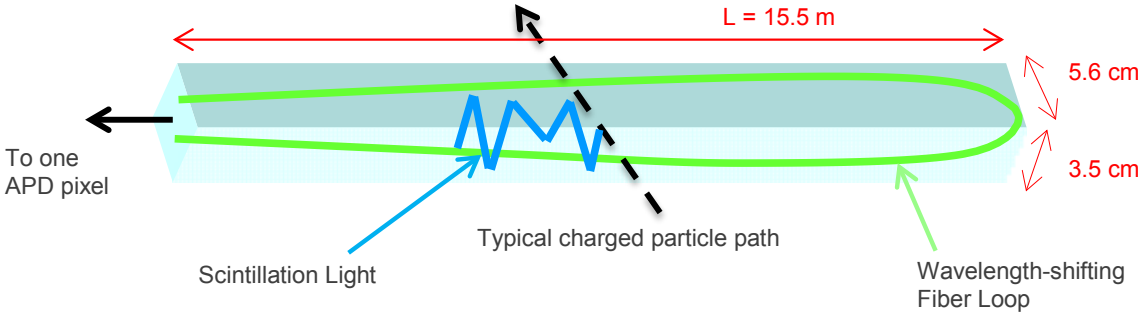

Figure 27: The fundamental unit cell of the detector of the NOνA near detector is shown. The cells are arranged in horizontal and vertical layers.

used to extract the light. This technology, called LiquidO, removes the need for manual segmentation: the lattice of fibres is constructed first and then the opaque scintillator poured in around the fibres. Substantially better spatial resolution per readout channel is achieved by utilizing the profile of the light detected across multiple fibres. Furthermore, the technology scales better in two ways. Firstly, to achieve more precise position resolution, e.g. in a voxelated detector reducing the fibre pitch by x2 requires x8 more cubic segments. Secondly, it scales better to larger masses: longer fibres can instrument more detector without needing more segments. Lastly, and importantly for DUNE $3^{rd}/4^{th}$ far detectors, the scintillator isotopic composition can be varied by exchanging the scintillator material, e.g. oil based scintillators can be swapped with water based ones. A design analogous to the T2K Super-FGD detector is envisaged for DUNE with the fibres running in all 3 perpendicular directions, allowing fine grained precision tracking and excellent calorimetry. The hydrogen-rich nature of organic or water-based scintillators as well as their fast timing provides a number of advantages for neutron measurements. In particular, greater stopping power and neutron time of flight measurements. The fast timing also allows measurements in a high-rate environment.

4.5 R&D and Engineering Road Map

R&D will be necessary for the Phase II Near detector, starting in 2024 and lasting for several years. It will be important to aim to fully define the detector requirements and have a conceptual design report in the late 2020s to be ready for construction in mid-2030s.

Some of the essential R&D and design work needed for the phase II near detector includes:

TPC charge readout and electronics test stands Charge readout TPCs are a mature technology with gas mixes identified that give sufficient gain. However, we must ensure that the full chain from amplification technology to readout electronics is tested in a high-pressure test stand to ensure adequate stability and gain in a non-flammable gas with a high argon fraction. Also, in choosing the gas, amplification technology, and readout electronics, the physics requirements need to be taken into account. With the right gas and amplification technology, the TPC can achieve a low energy threshold and get more

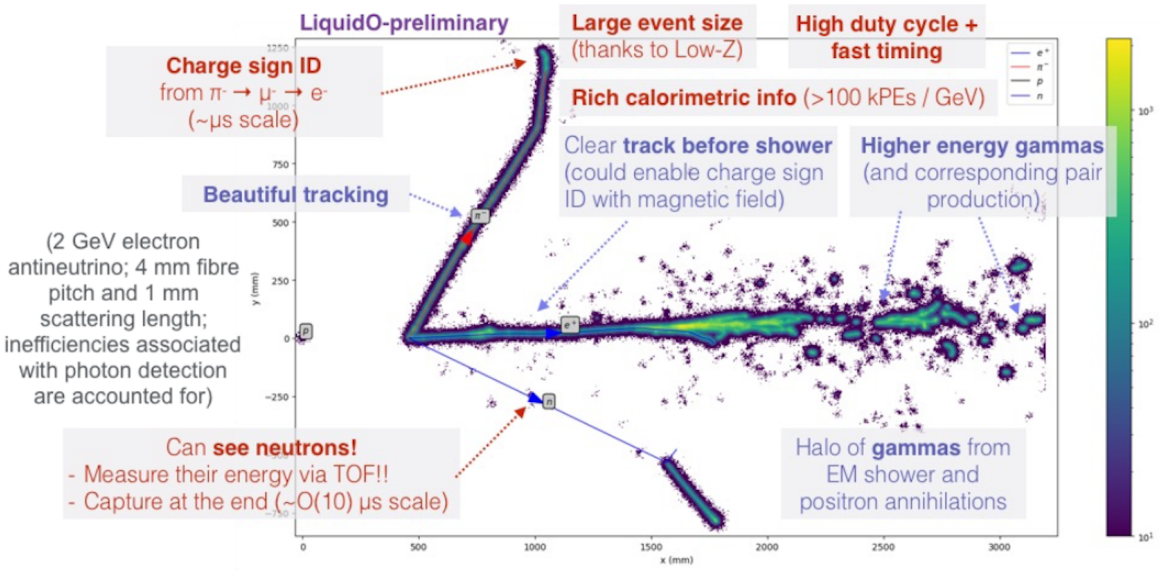

Figure 28: Annotated illustration of a 2 GeV electron neutrino interaction in a LiquidO-style ND.

detailed imaging of the hadronic activity at the neutrino interaction vertex. Additionally, the choice of the channel count in the readout electronics and the pixelization of the charge readout pads/strips play a role in the TPCs ability to lower the tracking threshold and achieve sub-mm point resolution.

Current testing has used wire chambers as the amplification stage, but with modern TPCs such as those for ALICE and sPHENIX using gas electron multipliers (GEMs) to achieve better stability of operation and higher gains we must also test this option. This work is ongoing in the UK (GEM work and readout electronics) and USA (readout electronics and test stands) using sources and test beams. A few examples include GEM Over-pressured with Reference Gases, GORG effort led by Indiana, testing a triple-GEM, and the Liverpool work described in Subsection 4.1.1.

Magnet INFN Genova is pursuing R&D on using magnesium diboride (MgB_2) superconducting cables which have a higher critical temperature and don't face some of the challenges of co-extruding NbTi superconducting cables with high-purity pure aluminium.

Light Detection The realization of light readout at the scale of the ND-GAr TPC poses important engineering challenges in relation to photosensor technology, HV integration, as well as the need of good light collection. Dedicated physics studies are needed to establish the best design path towards the optimization of the detection thresholds and time-tagging performance, and photosensor coverage. The readout options discussed above also both have R&D needed, for example low-temperature operation studies for SiPMs and operation at high pressure for LAPPDs. Groups in Spain (IGFAE-USC, UVigo, IFIC) are performing R&D on the optimization of the optical readout concept (required

coverage, use of reflectors and Winston Cones...)[50]. R&D on LAPPDs is also underway in the USA.

For amplification, the stability of proposed wavelength-shifting gases such as Ar/CF_4 (99/1) must be considered as they are low-quenched. Conventional GEM, thick-GEM, glass-GEMs, glass-Micromegas and wire chamber amplification stages are all currently under evaluation in Spain, the UK and the USA.

Finally, the outstanding tracking performance of the ND-GAr TPC needs to be guaranteed while securing that the photosensor plane is not blinded during the avalanche multiplication process in the anode region. This will require an additional R&D step targeting the minimization of photon-feedback, as it is customary for instance on RICH applications [54].

Calorimeter R&D was underway in Germany on coupling fibers to SiPMs to maximize light collection and uniformly illuminate SiPM face. Studies must also be done to optimize the calorimeter design, including the number of strip and tile layers, granularity, etc. A cost effective readout electronics system must also be developed.

Calibration Systems, Field Cage, and Gas Systems In addition to R&D on the magnet, light detection and charge collection systems, engineering work is also required to design the infrastructure and support services for the detector. The ALICE detector featured a high-performance TPC of a similar size [55], so some of that design can potentially be used as a starting point for ND-GAr. As an example, an essential requirement for accurate monitoring of drift velocity variations and inhomogeneities within the drift field is a laser calibration system that can uniformly illuminate the drift volume. This system must be closely aligned with the design of the high-voltage field cage. A new field cage and mechanical endcap structures will need to be constructed for ND-GAr TPC. Since the ND-GAr detector will be movable, a robust mechanical design for the field cage will be needed. A buffer region in between the field cage/photodetectors and pressure vessel will be needed to isolate the high voltage, and this may or may not require the use of an additional insulating gas. The detector performance depends crucially on the stability and quality of the gas in the drift region. For the DUNE HPgTPC system, we will need to develop the list of requirements on the control and stability of gas mixture in the drift gas mixture, and also the upper limits on O_2 and H_2O contaminant levels.

ND-LAr or SAND for phase 2 Is any major R&D needed here?

5 Summary

Glossary

anode plane a planar array of charge readout devices covering an entire face of a detector module. 14

anode plane assembly (APA) A unit of the horizontal drift detector module (FD1-HD) detector module containing the elements sensitive to ionization in the liquid argon (LAr). Each anode face has three planes of wires (two induction, one collection) to provide a 3D view, and interfaces to the cold electronics and photon detection system. 64

BDE bottom detector electronics. 12, 13

cold electronics (CE) Analog and digital readout electronics that operate at cryogenic temperatures. 12, 14

European Laboratory for Particle Physics (CERN) The leading particle physics laboratory in Europe and home to the ProtoDUNEs and other prototypes and demonstrators, including the Module 0s. 63, 66

conventional facilities (CF) Pertaining to construction and operation of buildings and conventional infrastructure, and includes cavern excavation. 64

charge readout (CRO) The system for detecting ionization charge distributions in a detector module. 13, 63

charge-readout plane (CRP) An anode technology using a stack of perforated PCBs with etched electrode strips to provide CRO in 3D; it has two induction layers and one collection layer; it is used in the FD2-VD far detector (FD) and dual-phase (DP) designs. 11, 13, 14, 16, 17, 63

charge-readout unit (CRU) In the FD2-VD design an assembly of the PCB panels plus adapter boards; two to a CRP. 13, 65

DOE U.S. Department of Energy. 65

dual-phase (DP) Distinguishes a liquid argon time-projection chamber (LArTPC) technology by the fact that it operates using argon in both gas and liquid phases; sometimes called double-phase. 63, 66

Deep Underground Neutrino Experiment (DUNE) A leading-edge, international experiment for neutrino science and proton decay studies; refers to the entire international experiment and collaboration. 2, 3, 11, 64–66

Experiment Hall North One (EHN1) Location at European Laboratory for Particle Physics (CERN) of the NP02 and NP04 areas used for the ProtoDUNEs and for other test and prototyping activities for DUNE. 65

far detector module The entire DUNE far detector design calls for segmentation into four modules, each with a total/fiducial mass of approximately 17 kt/10 kt. 65

far detector (FD) The 70 kt total (40 kt fiducial) mass LArTPC DUNE detector, composed of four 17.5 kt total (10 kt fiducial) mass modules, to be installed at the far site at Sanford Underground Research Facility (SURF) in Lead, SD, USA. 63, 65, 66

horizontal drift detector module (FD1-HD) LArTPC design used in FD1 in which electrons drift horizontally to wire plane anodes (anode plane assemblies (APAs)) that along with the front-end electronics are immersed in LAr. 63, 66

vertical drift detector module (FD2-VD) LArTPC design used in FD2 in which electrons drift vertically to PCB-based anodes at the top and bottom of the LAr volume, with a cathode in the middle. 13, 63–65

Fermi National Accelerator Laboratory (Fermilab) U.S. national laboratory in Batavia, IL. It is the laboratory that hosts Long-Baseline Neutrino Facility (LBNF) and DUNE, and serves as the experiment's near site. 65

field cage The component of a LArTPC that contains and shapes the applied E field. 11, 14

FRP fiber-reinforced plastic. 14

FS Depending on context, one of (1) the far site, SURF, where the DUNE far detector is located; (2) "Full Stream" relates to a data stream that has not undergone selection, compression or other form of reduction. 66

Far Site Conventional Facilities (FSCF) The conventional facilities (CF) at the DUNE far detector site, SURF, including all detector caverns and support infrastructure. 66

H2 CERN North Area hadron beamline used for ProtoDUNE-DP and FD2-VD prototypes and demonstrators. 65

H4 CERN North Area hadron beamline used for ProtoDUNE-SP and ProtoDUNE-SP-II. 65

horizontal drift single-phase, horizontal drift LArTPC technology. 66

high voltage (HV) Generally describes a voltage applied to drive the motion of free electrons through some media, e.g., LAr. 64

HVFT HV feedthrough. 14

HVPS high voltage (HV) power supply. 14

high voltage system (HVS) The detector subsystem that provides the time projection chamber (TPC) drift field. 14, 16

liquid argon (LAr) Argon in its liquid phase; it is a cryogenic liquid with a boiling point of 87 K and density of 1.4 g/ml. 63, 65, 66

liquid argon time-projection chamber (LArTPC) A TPC filled with liquid argon; the basis for the DUNE FD modules. 63, 64, 66, 67

Long-Baseline Neutrino Facility (LBNF) Long-Baseline Neutrino Facility; refers to the facilities that support the experiment including in-kind contributions under the line-item project. The portion of LBNF/DUNE-US responsible for developing the neutrino beam, the far site cryostats, and far and near site cryogenics systems, and the conventional facilities, including the excavations. 64

LBNF/DUNE-US Long-Baseline Neutrino Facility/Deep Underground Neutrino Experiment - United States; project to design and build the conventional and beamline facilities and the DOE contributions to the detectors. It is organized as a DOE/Fermi National Accelerator Laboratory (Fermilab) project and incorporates contributions to the facilities from international partners. It also acts as host for the installation and integration of the DUNE detectors. 65, 66

Module 0 The final pre-production instance of a detector; for the DUNE far detector modules, the ProtoDUNE-IIs in the 800 t cryostats in NP02 and NP04 serve this purpose. 63

NP02 The CERN North Area in Experiment Hall North One (EHN1) intersected by the H2 hadron beamline, the location of the 800 t cryostat used for ProtoDUNE-DP and for FD2-VD tests and prototypes; also used to refer to the 800 t cryostat in this area. 63, 65, 66

NP04 The CERN North Area in EHN1 intersected by the H4 hadron beamline, the location of ProtoDUNE-SP and ProtoDUNE-SP-II; also used to refer to the 800 t cryostat in this area. 63, 65, 66

PCB printed circuit board. 13, 63, 65

PCB panel In the FD2-VD design, one of four PCBs of size 1.5 × 1.7;m assembled into a CRU. 63

photon detector (PD) The detector elements involved in measurement of the number and arrival times of optical photons produced in a detector module. 16

photon detection system (PDS) The detector subsystem sensitive to light produced in the LAr. 14, 16

power-over-fiber (PoF) a technology in which a fiber optic cable carries optical power, which is used as an energy source rather than, or as well as, carrying data; this allows a device to be remotely powered, while providing electrical isolation between the device and the power supply. 16, 17

ProtoDUNE Either of the two initial DUNE prototype detectors constructed at CERN. One prototype implemented SP technology and the other DP. 63, 66

ProtoDUNE-DP The DP ProtoDUNE detector constructed at CERN in NP02. 11, 64, 65

ProtoDUNE-II The second run of a ProtoDUNE detector. 65

ProtoDUNE-SP The FD1-HD ProtoDUNE detector constructed at CERN in NP04. 11, 64, 65

ProtoDUNE-SP-II A second test run in the single-phase ProtoDUNE test stand at CERN, acting as a validation of the final single-phase detector design. 64, 65

quality assurance (QA) The process of ensuring that the quality of each element meets requirements during design and development, and to detect and correct poor results prior to production. 13

quality control (QC) The process (e.g., inspection, testing, measurements) of ensuring that each manufactured element meets its quality requirements prior to assembly or installation. 13

signal feedthrough chimney (SFT chimney) A volume above the cryostat penetration used for a signal feedthrough. 12

silicon photomultiplier (SiPM) A solid-state avalanche photodiode sensitive to single photoelectron signals. 16

signal-over-fiber (SoF) a technology in which a fiber optic cable carries detector output that has been converted from an electrical to an optical pulse. 16, 17

single-phase (SP) Distinguishes a LArTPC technology by the fact that it operates using argon in its liquid phase only; a legacy DUNE term now replaced by horizontal drift and vertical drift. 11, 66

Sanford Underground Research Facility (SURF) The laboratory in Lead, SD, USA where the DUNE FD will be installed and operated; also where the LBNF/DUNE-US Far Site Conventional Facilities (FSCF) and the FS cryostat and cryogenics systems will be constructed. 64

TDE top detector electronics. 11, 13

time projection chamber (TPC) Depending on context: (1) A type of particle detector that uses an E field together with a sensitive volume of gas or liquid, e.g., LAr, to perform a 3D reconstruction of a particle trajectory or interaction. The activity is recorded by digitizing the waveforms of current induced on the anode as the distribution of ionization charge passes by or is collected on the electrode. (2) TPC is also used in LBNF/DUNE-US for "total project cost". 64, 65

vertical drift single-phase, vertical drift LArTPC technology. 66

wavelength-shifting (WLS) A material or process by which incident photons are absorbed by a material and photons are emitted at a different, typically longer, wavelength. 16

References

[1] T. Nakada *et al.*, "The European Strategy for Particle Physics Update 2013. La stratégie européenne pour la physique des particules Mise à jour 2013. 16th Session of European Strategy Council,". https://cds.cern.ch/record/1567258.

[2] S. Ritz, H. Aihara, M. Breidenbach, B. Cousins, A. de Gouvea, M. Demarteau, *et al.*, "Building for discovery: strategic plan for us particle physics in the global context," *HEPAP Subcommittee* (2014) .

[3] **DUNE** Collaboration, V. Hewes *et al.*, "Deep Underground Neutrino Experiment (DUNE) Near Detector Conceptual Design Report," *Instruments* **5** no. 4, (2021) 31, arXiv:2103.13910 [physics.ins-det].

[4] **DUNE** Collaboration, B. Abi *et al.*, "Deep Underground Neutrino Experiment (DUNE), Far Detector Technical Design Report, Volume IV: Far Detector Single-phase Technology," *JINST* **15** no. 08, (2020) T08010, arXiv:2002.03010 [physics.ins-det].

[5] R. Ainsworth *et al.*, "Report from the Fermilab Proton Intensity Upgrade Central Design Group,".

[6] **DUNE** Collaboration, B. Abi *et al.*, "Deep Underground Neutrino Experiment (DUNE), Far Detector Technical Design Report, Volume II: DUNE Physics," arXiv:2002.03005 [hep-ex].

[7] A. Avasthi *et al.*, "Low Background kTon-Scale Liquid Argon Time Projection Chambers," in *Snowmass 2021*. 3, 2022. arXiv:2203.08821 [physics.ins-det].

[8] **DUNE** Collaboration, B. Abi *et al.*, "Supernova neutrino burst detection with the Deep Underground Neutrino Experiment," *Eur. Phys. J. C* **81** no. 5, (2021) 423, arXiv:2008.06647 [hep-ex].

[9] F. Pompa, F. Capozzi, O. Mena, and M. Sorel, "Absolute ν Mass Measurement with the DUNE Experiment," *Phys. Rev. Lett.* **129** no. 12, (2022) 121802, arXiv:2203.00024 [hep-ph].

[10] F. Capozzi, S. W. Li, G. Zhu, and J. F. Beacom, "DUNE as the Next-Generation Solar Neutrino Experiment," *Phys. Rev. Lett.* **123** no. 13, (2019) 131803, arXiv:1808.08232 [hep-ph].

[11] **DUNE** Collaboration, B. Abi *et al.*, "Prospects for beyond the Standard Model physics searches at the Deep Underground Neutrino Experiment," *Eur. Phys. J. C* **81** no. 4, (2021) 322, arXiv:2008.12769 [hep-ex].

[12] P. Ballett, T. Boschi, and S. Pascoli, "Heavy Neutral Leptons from low-scale seesaws at the DUNE Near Detector," *J. HEP* **111** (2020) , arXiv:1905.00284 [hep-ph].

[13] M. Breitbach, L. Buonocore, C. Frugiuele, J. Kopp, and L. Mittnacht, "Searching for physics beyond the Standard Model in an off-axis DUNE near detector," *JHEP* **01** (2022) 048, arXiv:2102.03383 [hep-ph].

[14] J. M. Berryman, A. de Gouvea, P. J. Fox, B. J. Kayser, K. J. Kelly, and J. L. Raaf, "Searches for Decays of New Particles in the DUNE Multi-Purpose Near Detector," *JHEP* **02** (2020) 174, arXiv:1912.07622 [hep-ph].

[15] K. J. Kelly, S. Kumar, and Z. Liu, "Heavy axion opportunities at the DUNE near detector," *Phys. Rev. D* **103** no. 9, (2021) 095002, arXiv:2011.05995 [hep-ph].

[16] P. Coloma, J. Martín-Albo, and S. Urrea, "Discovering Long-lived Particles at DUNE," arXiv:2309.06492 [hep-ph].

[17] W. Altmannshofer, S. Gori, M. Pospelov, and I. Yavin, "Neutrino Trident Production: A Powerful Probe of New Physics with Neutrino Beams," *Phys. Rev. Lett.* **113** (2014) 091801, arXiv:1406.2332 [hep-ph].

[18] P. Ballett, M. Hostert, S. Pascoli, Y. F. Perez-Gonzalez, Z. Tabrizi, and R. Zukanovich Funchal, "Z's in neutrino scattering at DUNE," *Phys. Rev. D* **100** no. 5, (2019) 055012, arXiv:1902.08579 [hep-ph].

[19] P. Ballett, M. Hostert, S. Pascoli, Y. F. Perez-Gonzalez, Z. Tabrizi, and R. Zukanovich Funchal, "Neutrino Trident Scattering at Near Detectors," *JHEP* **01** (2019) 119, arXiv:1807.10973 [hep-ph].

[20] W. Altmannshofer, S. Gori, J. Martín-Albo, A. Sousa, and M. Wallbank, "Neutrino Tridents at DUNE," *Phys. Rev. D* **100** no. 11, (2019) 115029, arXiv:1902.06765 [hep-ph].

[21] A. De Gouvêa, K. J. Kelly, G. V. Stenico, and P. Pasquini, "Physics with Beam Tau-Neutrino Appearance at DUNE," *Phys. Rev. D* **100** no. 1, (2019) 016004, arXiv:1904.07265 [hep-ph].

[22] A. Ghoshal, A. Giarnetti, and D. Meloni, "On the role of the ν_τ appearance in DUNE in constraining standard neutrino physics and beyond," *JHEP* **12** (2019) 126, arXiv:1906.06212 [hep-ph].

[23] J. Rout, S. Roy, M. Masud, M. Bishai, and P. Mehta, "Impact of high energy beam tunes on the sensitivities to the standard unknowns at DUNE," *Phys. Rev. D* **102** (2020) 116018, arXiv:2009.05061 [hep-ph].

[24] A. Lowe, K. Majumdar, K. Mavrokoridis, B. Philippou, A. Roberts, C. Touramanis, and J. Vann, "Optical Readout of the ARIADNE LArTPC using a Timepix3-based Camera," *arXiv e-prints* (Nov., 2020) arXiv:2011.02292, arXiv:2011.02292 [physics.ins-det].

[25] D. Hollywood, K. Majumdar, *et al.*, "ARIADNE—A novel optical LArTPC: technical design report and initial characterisation using a secondary beam from the CERN PS and cosmic muons," *Journal of Instrumentation* **15** no. 3, (Mar., 2020) P03003, arXiv:1910.03406 [physics.ins-det].

[26] A. Roberts, P. Svihra, *et al.*, "First demonstration of 3D optical readout of a TPC using a single photon sensitive Timepix3 based camera," *Journal of Instrumentation* **14** no. 6, (June, 2019) P06001, arXiv:1810.09955 [physics.ins-det].

[27] y. . . j. u. . h. P.Amedo et al, title = "Letter of Intent: Large-scale demonstration of the ARIADNE LArTPC optical readout system at the CERN Neutrino Platform".

[28] A. Lowe, K. Majumdar, K. Mavrokoridis, B. Philippou, A. Roberts, and C. Touramanis, "A novel manufacturing process for glass thgems and first characterisation in an optical gaseous argon tpc," *Applied Sciences* **11** no. 20, (2021) . https://www.mdpi.com/2076-3417/11/20/9450.

[29] A. Lowe, P. Amedo, *et al.*, "ARIADNE+: Large scale demonstration of fast optical readout for dual-phase LArTPCs at the CERN Neutrino Platform," *arXiv e-prints* (Jan., 2023) arXiv:2301.02530, arXiv:2301.02530 [physics.ins-det].

[30] A. Friedland and S. W. Li, "Understanding the energy resolution of liquid argon neutrino detectors," *Phys. Rev. D* **99** no. 3, (2019) 036009, arXiv:1811.06159 [hep-ph].

[31] D. Caratelli *et al.*, "Low-Energy Physics in Neutrino LArTPCs," arXiv:2203.00740 [physics.ins-det].

[32] P. Cennini *et al.*, "Improving the performance of the liquid argon TPC by doping with tetramethyl germanium," *Nucl. Instrum. Meth. A* **355** (1995) 660–662.

[33] **EXO-200** Collaboration, G. Anton *et al.*, "Measurement of the scintillation and ionization response of liquid xenon at MeV energies in the EXO-200 experiment," *Phys. Rev. C* **101** no. 6, (2020) 065501, arXiv:1908.04128 [physics.ins-det].

[34] **LArIAT** Collaboration, W. Foreman *et al.*, "Calorimetry for low-energy electrons using charge and light in liquid argon," *Phys. Rev. D* **101** no. 1, (2020) 012010, arXiv:1909.07920 [physics.ins-det].

[35] D. F. Anderson, "New Photosensitive Dopants for Liquid Argon," *Nucl. Instrum. Meth. A* **245** (1986) 361.

[36] **DUNE** Collaboration, N. Gallice, "Xenon doping of liquid argon in ProtoDUNE single phase," *JINST* **17** no. 01, (2022) C01034, arXiv:2111.00347 [physics.ins-det].

[37] E. P. Bernard *et al.*, "Thermodynamic stability of xenon-doped liquid argon detectors," *Phys. Rev. C* **108** no. 4, (2023) 045503, arXiv:2209.05435 [physics.ins-det].

[38] M. J. Dolinski, A. W. P. Poon, and W. Rodejohann, "Neutrinoless Double-Beta Decay: Status and Prospects," *Ann. Rev. Nucl. Part. Sci.* **69** (2019) 219–251, arXiv:1902.04097 [nucl-ex].

[39] A. Mastbaum, F. Psihas, and J. Zennamo, "Xenon-doped liquid argon TPCs as a neutrinoless double beta decay platform," *Phys. Rev. D* **106** no. 9, (2022) 092002, arXiv:2203.14700 [hep-ex].

[40] **T2K** Collaboration, K. Abe *et al.*, "T2K ND280 Upgrade - Technical Design Report," arXiv:1901.03750 [physics.ins-det].

[41] **T2K** Collaboration, D. Sgalaberna, "The T2K ND280 Upgrade," *PoS* **ICHEP2020** (2021) 175.

[42] C. Grupen, "Physics of particle detection," *AIP Conf. Proc.* **536** no. 1, (2000) 3–34, arXiv:physics/9906063.

[43] L. K. Emberger, *Precision Timing in Highly Granular Calorimeters and Applications in Long Baseline Neutrino and Lepton Collider Experiments*. PhD dissertation, Technische Universität München, School of Natural Sciences, 2022. http://d-nb.info/1278551751/34.

[44] F. Sefkow and F. Simon, "A highly granular SiPM-on-tile calorimeter prototype," *J. Phys.: Conf. Ser.* **1162** (2019) 012012, arXiv:1808.09281 [hep-ex].

[45] Z. Yuan, K. Briggl, H. Chen, Y. Munwes, H.-C. Schultz-Coulon, and W. Shen, "KLauS: A Low-power SiPM Readout ASIC for Highly Granular Calorimeters," in *2019 IEEE Nuclear Science Symposium and Medical Imaging Conference (NSS/MIC)*, pp. 1–4. 2019.

[46] K. Saito, H. Tawara, T. Sanami, E. Shibamura, and S. Sasaki, "Absolute number of scintillation photons emitted by alpha particles in rare gases," *IEEE Trans. Nucl. Sci* **49** (2002) 4.

[47] R. Santorelli, E. Sánchez García, P. García Abia, D. González-Díaz, R. Lopez Manzano, J. J. Martínez Morales, V. Pesudo, and L. Romero, "Spectroscopic analysis of the gaseous argon scintillation with a wavelength sensitive particle detector," *Eur. Phys. J. C* **81** (2021) 622.

[48] D. González-Díaz, F. Monrabal, and S. Murphy, "Gaseous and dual-phase time projection chambers for imaging rare processes," *Nucl. Instr. Meth. A* **878** (2018) 200–255.

[49] P. Amedo, S. Leardini, A. Saá-Hernández, D. González, and D. González-Díaz, "Primary scintillation yields of α particles in pressurized Argon-CF_4 mixtures," *in preparation, preliminary results in LIDINE 2021, https://indico.physics.ucsd.edu/event/1/contributions/62/* .

[50] A. Saá-Hernández, D. González-Díaz, J. Martín-Albo, M. Tuzi, P. Amedo, and S. Leardini, "On the determination of the interaction time of GeV neutrinos in large argon gas TPCs," *submitted to JHEP* .

[51] P. Amedo, D. González-Díaz, F. M. Brunbauer, D. Fernández-Posada, E. Oliveri, and L. Ropelewski, "Observation of strong wavelength-shifting in the argon-tetrafluoromethane system," *submitted to Frontiers in Detector Science and Technology* , arXiv:2306.09919 [physics.ins-det].

[52] M. D'Incecco, C. Galbiati, G. K. Giovanetti, G. Korga, X. Li, A. Mandarano, A. Razeto, D. Sablone, and C. Savarese, "Development of a Novel Single-Channel, 24 cm^2, SiPM-Based, Cryogenic Photodetector," *IEEE Trans. Nucl. Sci.* **65** no. 1, (2018) 591.

[53] R. L. Talaga, J. J. Grudzinski, S. Phan-Budd, A. Pla-Dalmau, J. E. Fagan, C. Grozis, and K. M. Kephart, "PVC Extrusion Development and Production for the NOvA Neutrino Experiment," *Nucl. Instrum. Meth. A* **861** (2017) 77–89, arXiv:1601.00908 [physics.ins-det].

[54] M. Blatnik *et al.*, "Performance of a Quintuple-GEM Based RICH Detector Prototype," *IEEE Trans. Nucl. Sci.* **62** no. 6, (2015) 3256–3264, arXiv:1501.03530 [physics.ins-det].

[55] J. Alme *et al.*, "The ALICE TPC, a large 3-dimensional tracking device with fast readout for ultra-high multiplicity events," *Nucl. Instrum. Meth. A* **622** (2010) 316–367, arXiv:1001.1950 [physics.ins-det].